Dynamic integrated ground vehicle and drone routing with simultaneous surveillance coverage for evading intentional disruption

Fatemeh Zandieh [a], Seyed Farid Ghannadpour [b,1], Mohammad Mahdavi Mazdeh [c]

[a] Department of Industrial Engineering, Iran University of Science and Technology, Iran, 16846-13114.
Email: fatemeh_zandiyeh@ind.iust.ac.ir

[b] Department of Industrial Engineering, Iran University of Science and Technology, Iran, 16846-13114.
Email: ghannadpour@iust.ac.ir
Tel: (+9821)-73225015

[c] Department of Industrial Engineering, Iran University of Science and Technology, Iran, 16846-13114.
Email: mazdeh@iust.ac.ir
Tel: (+9821)-73225002

Corresponding author (✉)
Permanent Address: Department of Industrial Engineering, Iran University of Science and Technology, Tehran, Iran, 16846-13114.
Tel.: +98 21 73225015;
Email: ghannadpour@iust.ac.ir

Dynamic integrated ground vehicle and drone routing with simultaneous surveillance coverage for evading intentional disruption

Abstract

The purpose of this study is to examine the use of drones to provide transportation security during times of intentional disruption. Due to the nature of valuable goods, their transportation is always associated with certain risks, necessitating implementing security measures to ensure the transportation process's security. This study aimed to address the security of valuable goods transportation by proposing a new routing problem using drones termed integrated routing and surveillance (IRS) for ground and aerial vehicles operating in dynamic environments. This approach addresses the issue of deliberate disruption at the planning and implementation phases. Risks are estimated during the planning phase using historical data, and routing is designed to minimize risk and travel costs. Drones conduct online surveillance of the solution routes generated during the planning phase throughout the implementation phase. Ground vehicles are not permitted to enter a link unless drones assess the risks prior to their entry. Drones' arrival times for this assessment of each ground link are determined by non-predefined time windows. Drones can visit multiple ground links if their time windows overlap in the proposed problem. If the drones detect a suspicious agent, they will perform dynamic replanning to avoid the risk source. Additionally, the proposed problem is optimized using new ALNS (adaptive large neighborhood search) and SA-based (simulated annealing) algorithms. The proposed algorithm's efficiency and effectiveness are evaluated for small and large cases. The results demonstrate the proposed model's applicability and superiority to ALNS.

Keywords: vehicle routing problem, surveillance drone, risk management, intentional disruption, cash-in-transit, ALNS

1. Introduction

Nowadays, unmanned aerial vehicles (UAVs) or drones have been widely adapted for various real-world applications. Drones are becoming more popular due to their ability to record video directly and capture images in real-time and their ability to fly and transport goods. They can be employed in various non-military applications, including surveillance, transportation, environmental monitoring, the surveillance industry, agricultural services, and disaster recovery. Drones can also be utilized for military purposes such as air exploration, battlefield surveillance, target localization,

tracking, damage assessment, and arresting criminals. Drones are well-known for their fundamental advantages, including mobility, adjustable height, effortless landing, and flexibility.

Security and surveillance are two rapidly growing fields where drones are being used. Surveillance drones are unmanned aerial vehicles used to capture still images and video or live video from specific targets such as vehicles or specific locations. Drone surveillance is a simple, quick, and cost-effective method of gathering data. Additionally, they can be equipped with night-vision cameras and thermal sensors that enable them to detect images that are invisible to the naked eye. As a result, governments, military, law enforcement, and businesspeople may employ drones to collect data that assists them in making decisions (Nichols, 2020). Moreover, using drones for surveillance enables access to regions inaccessible to humans or ground vehicles. The majority of drones are quieter, less expensive, and capable of flying at lower altitudes than manned aircraft.

Drones use real-time control stations to deploy eyes on specific regions rapidly. To this end, they have a critical advantage in that they can collect images, facilitate rapid identification, and increase awareness of a situation, and ground force units can use them to identify potential surveillance threats from a safe distance.

Because valuable goods and cash are intrinsically disruptive, their transportation is associated with intentional disruption. Disruption is defined as preventing a task, a trend, or a process from a system's normal state or expectation. In other words, when a system adheres to several predefined targets, an agent makes deliberate choices and takes actions that affect other facts. Intentional disruption of valuable goods or cash transportation includes attacks and armed robbery. As a result, one of the primary concerns of CIT (cash-in-transit) companies is to minimize their exposure to robbery. Under disruption conditions in the transportation of valuable goods, two major approaches to identifying and forecasting robbery risk can be taken. In most risk management studies, the risk of robbery is estimated using historical data on transportation routes.

In this research, risk management is conducted through surveillance via drones. Suspected cases, such as guns and armed men, can be identified through continuous and dynamic surveillance by drones along transportation routes, and robbery can be predicted before it occurs by notifying the control center and rerouting the route. Thus, this study proposes the IRS routing problem for integrating ground vehicles and drones used to transport valuable goods. In this model, valuable goods are transported via ground vehicles (vans) whose routes are monitored by drones. Furthermore, the dynamic simulated annealing & adaptive large neighborhood search (D-SALNS) algorithm optimizes the problem and generates competitive solutions.

This study is organized as follows: Section 2 summarizes the literature review results to identify critical issues and research gaps. Section 3 contains the IRS model's mathematical modeling. Section 4 is dedicated to the design of the D-SALNS algorithm. Section 0 analyzes and validates the solution algorithm's output. Finally, Section 6 summarizes the study's major findings and concludes the paper.

2. Literature review

This section presents a literature review in two subsections, namely, the routing problem with drones and valuables routing problem.

2.1. Routing problem with drones

The routing problem with drones has piqued researchers' interest in recent years. Dorling et al. (2016) introduced the drone routing problem (DRP) to minimize fuel consumption costs and mitigate time constraints. They used the simulated annealing (SA) algorithm to optimize their proposed model. Coelho et al. (2017) also considered a heterogeneous drone routing problem with seven objective functions in a dynamic environment. Their proposed model's objective function included minimizing total traveled distance, total drone delivery time, total drone usage, total drone speed, makespan of the last collected and delivered package, and the maximization of battery level until the end of planning. Alotaibi et al. (2018) suggested a UAV routing problem for determining UAV routes to military target locations. Additionally, they accounted for threat exposure and travel time in their model and generated a waypoint using a maxi-min approach to minimize the risk of encountering threat spots. The objective function of the proposed model was to maximize the number of visited target locations.

Liu (2019) proposed a real-time routing problem for distributing and collecting meals in a dynamic operational environment and a heuristic algorithm based on mixed integer planning (MIP) to aid decision-making in an infinite horizon. Song et al. (2018) proposed a UAV routing problem using mixed-integer linear planning (MILP). Zhen et al. (2019) proposed a UAV routing problem to monitor certain regions on Earth. Additionally, the authors considered the height of UAVs as a decision variable that influences service accuracy and duration in the study. Semiz and Polat (2020) used a vehicle routing problem to monitor target regions with drones over a period of time. The objective functions included minimizing distance, time window constraints, and fuel consumption.

Several studies employ a combination of ground vehicles and drones to provide customer service. Wang et al. (2017) introduced the VRP-D problem, which involves the delivery of packages to customers by transportation systems, including trucks equipped with drones. Drones may depart from trucks stationed at a depot or a customer's location and return to the exact location after their service. Delivering packages via trucks is also possible, but trucks must be stationed at delivery locations during drone launch and pickup. Poikonen et al. (2017) proposed the VRP-D problem, in which one drone is launched from each truck and returns to the truck after delivering a package to a customer to recharge or change the battery. Trucks can also be used to deliver packages, but they must be stationed at delivery locations or depots during the launch or landing of drones. The authors defined the objective function as minimizing package delivery time.

Sacramento et al. (2019) also proposed a vehicle routing problem involving drones, in which a drone takes off from a truck and returns to the same truck after servicing a single customer. Customers affected by this issue are divided into two categories: those who require heavy delivery and can only be met by truck and those whose demand can be met by drone and truck.

Schermer et al. (2019b) proposed a vehicle routing problem in drones, in which each truck transports multiple drones for customer service to minimize makespan. They modeled the problem using the MILP technique. Schermer et al. (2019a) also presented a work similar to Schermer et al. (2019b), except that the drones return to distinct locations in each link rather than trucks. Karak and Abdelghany (2019) developed a collection and delivery service with a combined vehicle-drone routing problem. The proposed model's objective function was cost minimization.

Kitjacharoenchai et al. (2020) advanced the concept of a bi-level VRP-D. According to their proposed model, some customers receive service from trucks, while others receive service from drones, with trucks departing the depot to provide service to customers. Furthermore, drones fly from trucks and return to the same truck after providing service to customers. Li et al. (2020) proposed a bi-level drone-van routing problem with time windows and multiple drones in each van. At the first level, packages are distributed via vans; at the second level, packages are distributed via drones. Dayarian et al. (2020) presented a vehicle routing problem with resupplying goods via drone in dynamic environments where drones are used to resupply delivery trucks to model the home delivery system.

Gu et al. (2020) designed a carrier vehicle problem with drones (CVP-D). Initially, their proposed problem established the ground vehicle stop. Then, customers were assigned to the ground vehicle and drone stop locations. The final step was to determine the routes of ground vehicles and drones. Poikonen and Golden (2020b) expanded on the model proposed by Poikonen et al. (2017). In their study, drones launched from trucks were shown to deliver various heterogeneous packages to customers. Additionally, the battery life of drones depended on the weight of packages. Poikonen and Golden (2020a) considered two types of mothership vehicles in the CVP-D problem: mothership vehicles (large vehicles such as planes and ships) and drone vehicles (small vehicles such as drones and boats). Drones took off from the mothership and returned after visiting several refueling targets.

In the VRP-D problem proposed by Euchi and Sadok (2021), drones' speed was prioritized over ground vehicles, and each flight supplies a single customer's demand. The launch and return points of the drone from and to ground vehicles were not identical. The authors expressed the proposed model as a MILP and used CPLEX to solve small-size instances. Moreover, they used the genetic algorithm to solve problems of a large size. Tamke and Buscher (2021) modeled the VRP-D problem using two time-oriented MILP objective functions. The first objective function sought to minimize makespans, which were accomplished using the min-sum VRP-D algorithm. The second objective function ensured justice by balancing route lengths, accomplished via min-max VRP-D. Furthermore, the authors used branch and cut (BAC) optimization to fine-tune the proposed model. Boccia et al. (2021), Kuo et al. (2022), Lei et al. (2022), and Ermağan et al. (2022). Table 1 summarizes the problems discussed in this section.

Table 1. A review of routing problem with drones

References	Problem type	Objective function(s)	Drone application		dynamic	Time windows	Case study
			monitoring	delivery and/or collection			
Dorling et al. (2016)	DRP	DTM, TCM		✓			Delivery and emergency response
Coelho et al. (2017)	DRP	TDM, TTM, MNUV, UMSM, MMLCP, MMLDP, BLM		✓	✓		Crisis management
Wang et al. (2017)	VRP-D	CTM		✓			Distribution system
Poikonen et al. (2017)	VRP-D	CTM, TCM		✓			Distribution system
Alotaibi et al. (2018)	DRP	MNVC	✓				Enemy detection in a military environment
Song et al. (2018)	DRP	MNVC, TDM		✓		✓	Distribution system
Liu (2019)	DRP	ES, ML, ME		✓	✓		Meal delivery service
Zhen et al. (2019)	DRP	TTM	✓				-
Sacramento et al. (2019)	VRP-D	OCM		✓			Distribution system
Schermer et al. (2019a)	VRP-D	MM		✓			Distribution system
Schermer et al. (2019b)	VRP-D	MM		✓			Distribution system
Karak and Abdelghany (2019)	CVP-D	TCM		✓			Distribution and collection system
Wang and Sheu (2019)	VRP-D	TCM		✓			Distribution system
Semiz and Polat (2020)	DRP	TDM	✓				-
Kitjacharoenchai et al. (2020)	VRP-D	CTM		✓			Distribution system
Li et al. (2020)	VRP-D	TCM		✓		✓	Distribution system
Dayarian et al. (2020)	TSP-D	MPOS, TC		✓	✓		Distribution system
Gu et al. (2020)	CVP-D	MNUV		✓			Distribution system
Poikonen and Golden (2020b)	CVP-D	CTM		✓			Distribution system
Poikonen and Golden (2020a)	CVP-D	CTM		✓			Distribution system
Euchi and Sadok (2021)	VRP-D	TTM		✓			Distribution system
Tamke and Buscher (2021)	VRP-D	MM		✓			Distribution system
Boccia et al. (2021)	TSP-D	TTM		✓			Distribution system
Kuo et al. (2022)	DRP	TTM	✓		✓		precision agriculture, search and rescue, and military surveillance
Lei et al. (2022)	VRP-D	OCM		✓			Distribution system
Ermağan et al. (2022)	VRP-D	TCM		✓		✓	Distribution system
This study	IRS	TCM, TRM	✓		✓	✓	Cash and valuables-in-transit

DTM: Delivery Time Minimization, TCM: Travel Cost Minimization, TDM: Travel Distance Minimization, TTM: Travel Time Minimization, , MNUV: Minimization of Number of Used Vehicle, UMSM: UAV Maximum Speed Minimization, MMLCP: Minimization of Makespans of the Last Collected Package, MMLD: Minimization of Makespans of the Last Delivered Package, BLM: battery Load Minimization, CTM: Completion Time Minimization MNVC: Maximization of Number of Visited Customer, ES: Ensure Safety, ML: Minimize Lateness, ME: Maximize Efficiency, OCM: Operation Cost Minimization, MM: Makespan Minimization, MPOS: Maximization of Percentage of Orders Serve, TSP-D: Travelling Salesman Problem with Drones, TCRM: Total Risk Minimization.

2.2. Valuables routing problem

Transportation risk is a significant factor to consider in studies on valuable goods routing problems. One strategy for enhancing transportation security is to create unpredictable routes.

Ngueveu et al. (2009, 2010, 2013) proposed a new approach termed m-peripatetic, in which it is prohibited to use each link more than once during an m-period. Additionally, the amount of cash that can be carried in each vehicle is limited. Yan et al. (2012) increased transportation security through route unpredictability by utilizing the time-space technique. These techniques generate more flexible and secure routes based on time and space similarity in routing and scheduling. Michallet et al. (2014) also created dissimilar routes across periods by altering how services are delivered to customers. This study alters the customer arrival time for each period to generate dissimilar routes.

Talarico et al. (2015a) reduced the risks associated with cash transportation by generating k-dissimilar routes. To this end, the authors proposed a new index for calculating the similarity of solutions and then generated dissimilar routes using it. Constantino et al. (2017) proposed a cash distribution arc routing problem in which the security of cash transportation is increased by changing tours on consecutive days. Hoogeboom and Dullaert (2019) also proposed a vehicle routing problem with multiple cash distribution time windows, in which unpredictable routes are generated by diversifying the arrival times of vehicles to each customer. Additionally, Soriano et al. (2020) created a routing problem with time windows the varying arrival times for cash transportation and generated unpredictable solutions at various times by minimizing the difference between arrival times and each customer. Moreover, a multi-node network is used to generate more diverse solutions.

Furthermore, to mitigate cash transportation risk, Talarico et al. (2015b) introduced a new type of VRP problem called the risk-constrained cash-in-transit vehicle routing problem (RCTVRP). The addition of one constraint to the VRP problem limited cash transportation risk based on maximum insurance coverage. In another study, Talarico et al. (2017b) optimized the RCTVRP problem using the ant colony optimization with a large neighbourhood search (ACO-LNS) algorithm. Using RCTVRP, Radojičić et al. (2018) reduced the risk of cash transportation and resolved the problem by developing a fuzzy greedy randomized adaptive search procedure based on path relinking. Xu et al. (2019) proposed a multi-product RCVRP in which different cash denominations were considered for each customer demand (bank branch, ATM, supermarket).

Another type of cash routing problem generates solutions with a high degree of security by estimating link risks and minimizing risk. Talarico et al. (2017a) proposed a bi-level model for minimizing the cost and risk of cash transportation. They optimized the problem using progressive multi-objective optimization with iterative local search (PMOO-ILS). In addition to risk estimation, reduced repeatability of links is addressed in several other studies. Furthermore, Bozkaya et al. (2017) proposed a bi-objective model for reducing risk and cost in transporting valuable goods. Moreover, the authors defined a combined risk based on the weighted total number of times a link is used and the socioeconomic status of the routes' surrounding regions.

Ghannadpour and Zandiyeh (2020b) proposed a vehicle routing problem with time windows for cash transportation to minimize risk and distance, in which a games theory approach is used to estimate the possibility of robbery. For the unpredictability of transportation links, the authors also

considered the robbery probability dependent on the number of times a link is used. In another study, Ghannadpour and Zandiyeh (2020a) proposed a useful good routing problem with time windows and two objective functions: risk minimization and distance minimization. The study considered the risk of robbery concerning the possibility of robbery, the probability of successful robbery, the amount of transported goods, the length of the link, and the number of consecutive uses of the link.

Tikani et al. (2020) proposed a periodic multi-objective routing problem with a multi-graph for cash transportation to minimize time and cost while maximizing customer satisfaction. Additionally, they generated unpredictable alternative routes by varying each customer's arrival time. Tikani et al. (2021) posed a cash transportation routing problem under the assumption of time-dependent and possibly congested traffic. They modeled the problem as a multi-node network with specific risks and travel times for each link. Furthermore, they optimized the problem by developing a new algorithm based on flexible restricted dynamic programming and a self-adaptive caching genetics algorithm. Other studies in this field include Fallahtafti et al. (2021), (Allahyari et al., 2021b), and (Allahyari et al., 2021a).

Most previous research on drone routing issues has concentrated on commercial applications and efficient transportation. Although surveillance drones have a wide variety of applications in various fields, they have only been studied and developed in a limited number of studies. One of these fields in which surveillance drones can be beneficial and improve performance is distributing valuable goods and preventing intrinsic intentional disruption. Developing and implementing such an approach is also recommended in several valuable good transportation companies (PIANA, 2017). Problem novelties in the current study are listed as follows:

- Proposing a novel method of coordination between ground and aerial vehicles
- Utilizing drone surveillance to assess the risk posed by an intentional disruption of the transportation system
- For the first time in this study, a new procedure for risk management in valuable goods transportation is proposed, in which a reactive response to risk is proposed and a proactive response to risk.

  Consider the possibility of overlapping time windows for the simultaneous visit of a drone via two or more ground links
- Developing problem-solving algorithms by combining them with heuristic and meta-heuristic algorithms

3. Integrated routing and surveillance model

In this case, drones are used to monitor ground vehicle routes in order to protect the transportation of valuable goods (cash) from intentional disruptions. As a result, optimization and risk mitigation is accomplished in two phases: planning and implementation. The planning phase proposes

integrated routing and surveillance (IRS) model. First, based on historical data about the problem, a solution with the lowest possible drone and ground vehicle costs (travel cost and risk) is identified. Drones monitor and control routes prior to ground vehicle travel during the implementation phase (modeled in Section 3.1). The security control room (SCR) will be notified if drones identify hazards along the routes of ground vehicles. Following that, problem risk data is updated. Reoptimization is used to eliminate risk links from ground vehicle routes by rerouting service routes (details in Sections 3.3). This process is repeated until all cash is distributed among banks, as illustrated in Fig. 1.

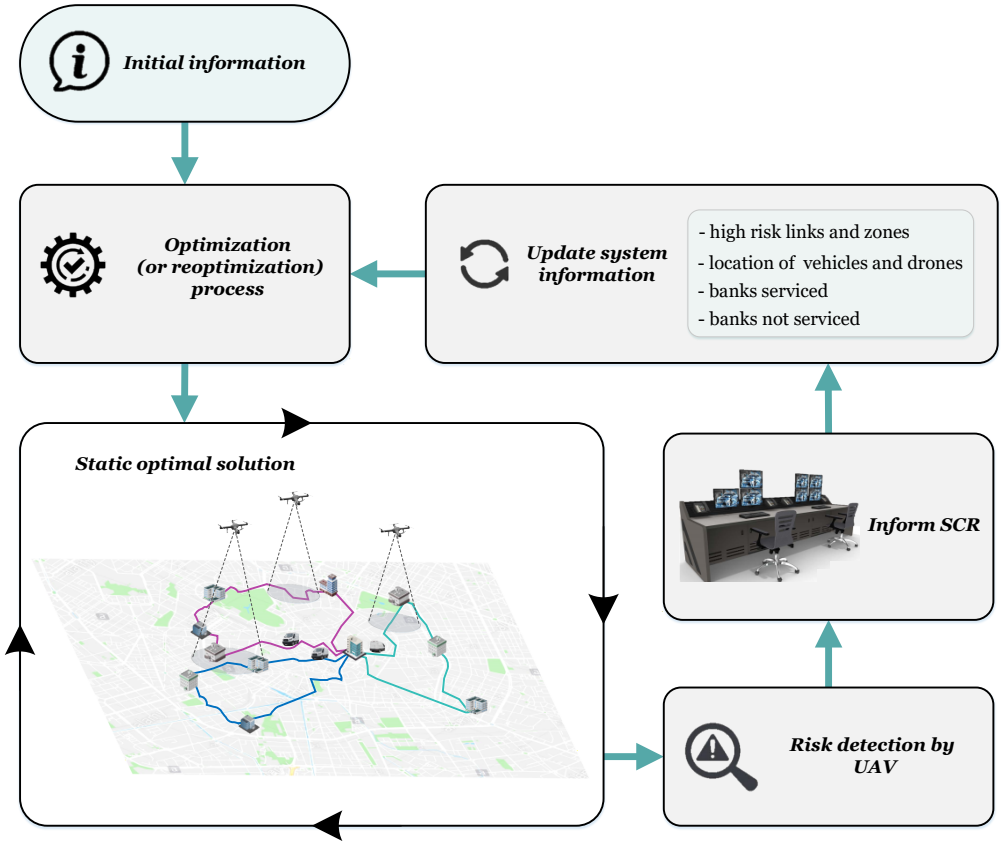

Fig. 1. Conceptual model of the proposed problem

3.1. Mathematical modeling

The IRS issue is comprised of N bank branches and $N^{'}$aerial zone centers. $C = \{0,1,2,..., N\}$ denotes bank branch sets, with node 0 denoting the central treasury. Cash transfers are made via a network of ground vehicles denoted by the letters $K = \{1,2,...,| K|\}$. Ground vehicle k carrying D_{0j}^{k} load departs from the central treasury and returns after distributing cash to bank branches. Due to intentional disruptions in cash transportation, a collection of drones denoted by $A = \{1,2,...,| A|\}$ is used to ensure security. Drones depart from the aerial zone's center, denoted by $\mathcal{C} = \{0,1,2,..., N^{'}\}$ (node 0 indicates the central treasury), and they monitor and control the covered ground routes for $\pi_{i'}$. Additionally, drones fly at varying altitudes depending on the ground conditions. Flight

altitudes affect the drone's radius and control precision. Thus, flight altitude is calculated as a parameter in accordance with technical specifications, constraints, and environmental conditions. Fig. 2 illustrates the various flight altitudes of drones in various regions. Additionally, the figure depicts the zones (perimeter circle) and area (enclosed square).

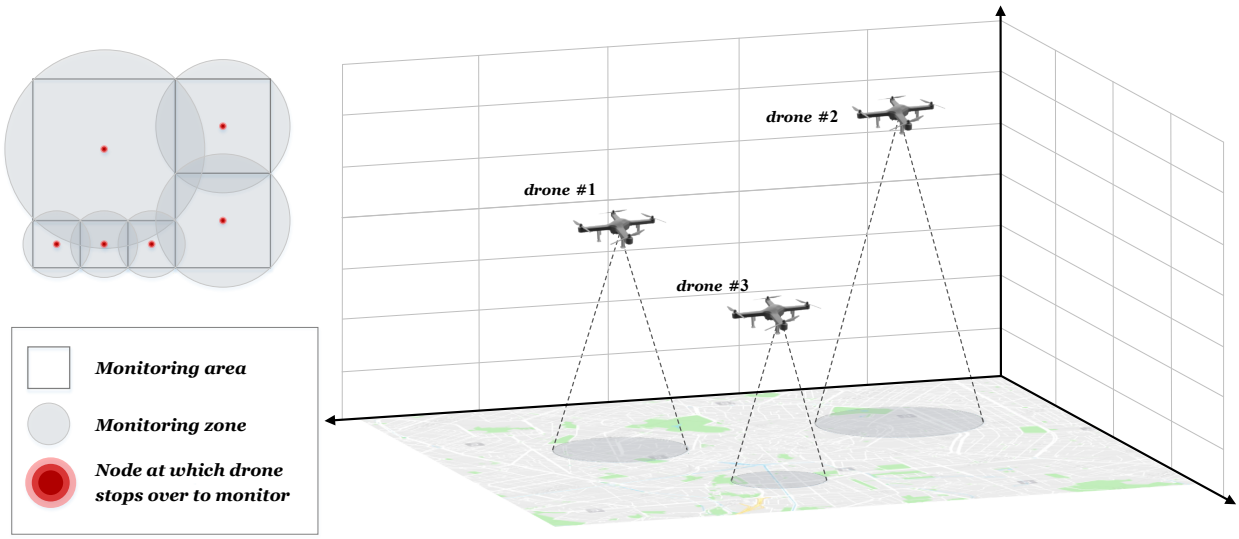

Fig. 2. Drones flight altitude and their control radius

A hypothetical example of city zoning for cash transportation control is shown in Fig. 3 to illustrate control by drones more clearly. Each aerial zone center can cover and secure one or more links and vice versa, meaning that each link can also be controlled and secured by one or more aerial zone centers, depending on its length. $z_{ij}^{i'}$ is a binary parameter that represents the relationship between the aerial zone center i' and the link ij. If the aerial zone center i' covers the link ij, parameter $z_{ij}^{i'}$ will equal 1; if not, it will equal 0.

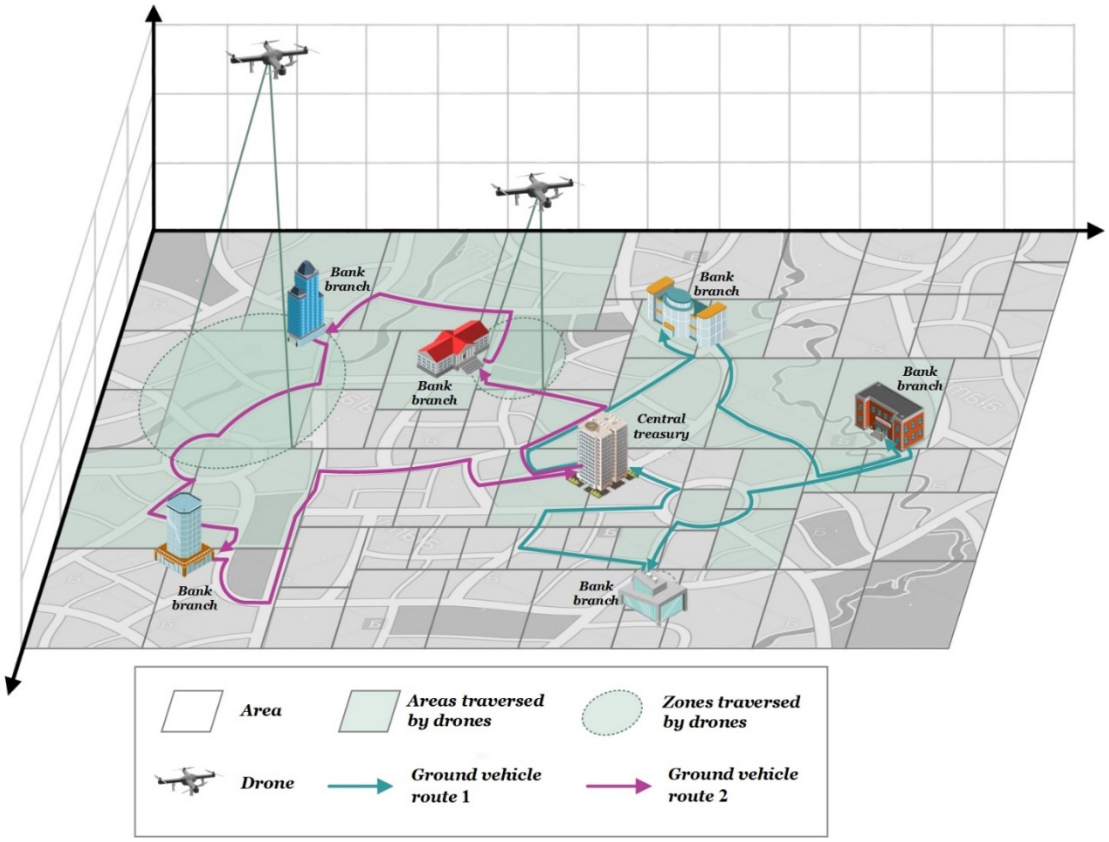

Fig. 3. Ground vehicle routes and control procedure via a hypothetical example

According to Fig. 3, drones monitor and control ground vehicle routes. Drone route planning may be configured so that one or more drones can control each link, depending on the number of aerial zone centers that cover it. Fig. 4 illustrates various drone routings in which one to four drones may be used to surveil a link. In Fig. 4 (a), a drone monitors four aerial zones that pass link 0-1. Two drones are used in Fig. 4 (b) to monitor the aerial zones of link 0-1. Three and four drones are used to monitor this link, respectively, in the planning and routing depicted in Fig. 4 (c) and (d).

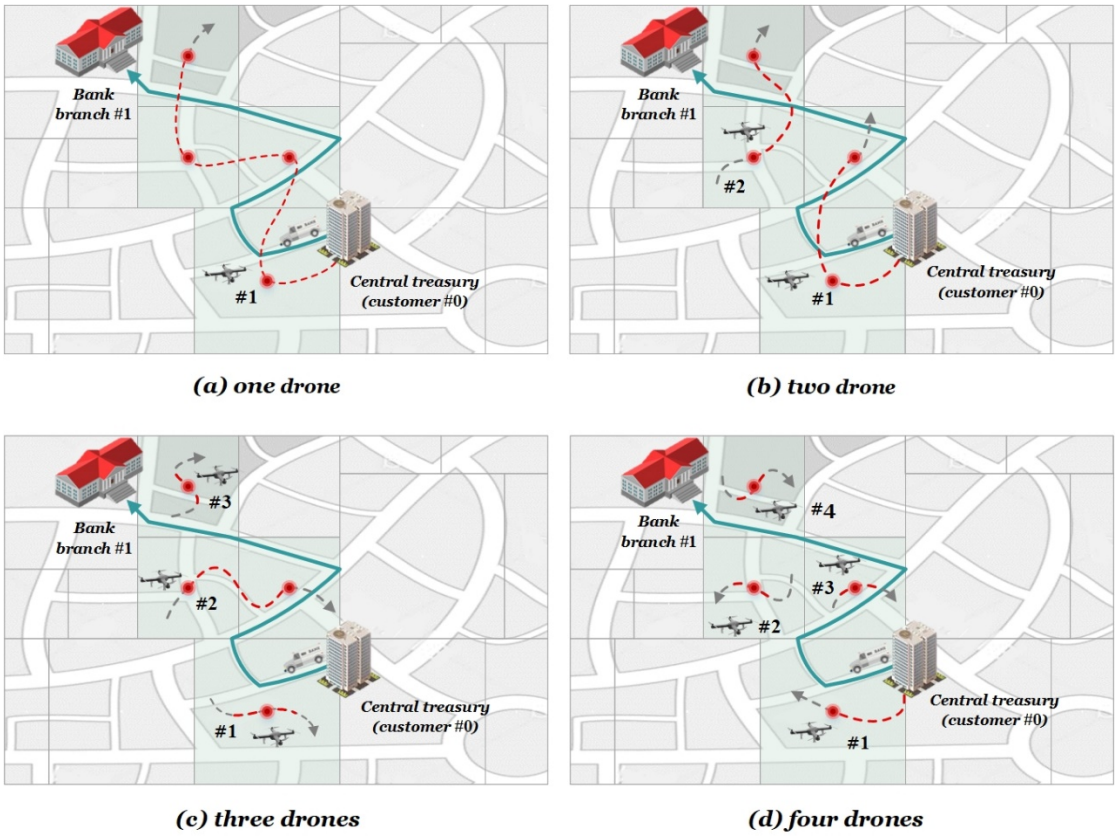

Fig. 4. Different planning for drone surveillance on a link traversed by a ground vehicle

Drones control and assess the bank's outlet link's security to monitor transportation routes during a specific period (time window) before a ground vehicle leaves a bank. e_i and l_i variables are defined to model this concept and to define the beginning and end of this time window, which indicate the earliest time to ensure the security of the output link from bank i via drone and the exit time of the ground vehicle from bank i. l_i variable is calculated through the sum of arrival time to bank i (at_i) and service time to the bank i (f_i) via formula (1). The relationship between e_i and l_i is determined by the Δ_i parameter. Accordingly, the earliest time to ensure exit from bank i equals to Δ_i the time before the ground vehicle leaves bank i. e_i variable is calculated via formula (2).

$$at_i + f_i = l_i \qquad \forall i \in C \backslash \{0\} \qquad (1)$$

$$l_i - \Delta_i = e_i \qquad \forall i \in C \qquad (2)$$

As previously stated, if a threat exists in a link, re-optimization will occur, and routes will change. As a result, re-optimization takes a short time, and the latest time for drone surveillance on the zone-covering link cannot be equal to the time for bank i's ground vehicle to exit or the time for an outbound link to begin moving i (l_i). To this end, the δ_i parameter is defined, which is referred to as the reset or re-optimization time. Thus, δ_i is the minimum time required before ground vehicles can enter the outlet link from i via controlled drones. Thus, an outbound link from i equals

$[e_i, l_i - \delta_i]$ and covers the time window or drone movement of each aerial zone center. Thus, the drone's movement must be adjusted to arrive at the aerial zone center i' at time $[e_i, l_i - \delta_i]$ (aerial zone center i' over link begins from i) to ensure the outbound link's security from bank i. Otherwise, that link cannot be entered by a ground vehicle.

Each aerial zone is only visited once in order to control a link. Additionally, each drone is only permitted to pass through each aerial zone center once. Although an aerial zone center can cover multiple ground links, each ground link is defined by a single time window. If the time windows of links passing through the center of an aerial zone overlap, drones can surveil two or more links from that aerial zone. A shared time window is created in this case. Fig. 5 (a) illustrates how time windows overlap in the outbound link from bank 1 ($[e_1, l_1 - \delta_1]$) and the outbound link from bank 4 ($[e_4, l_4 - \delta_4]$) during surveillance on links 4-3 and 1-2. Furthermore, if the time windows for outbound links from banks 1 and 4 do not overlap, a multiple-time window for aerial zone center 5 is created, and a drone independently monitors each link. Fig. 5 (b) depicts a scenario in which drone #1 and drone #2 in aerial zone center five visits and assess the security of links 1-2 and 4-3.

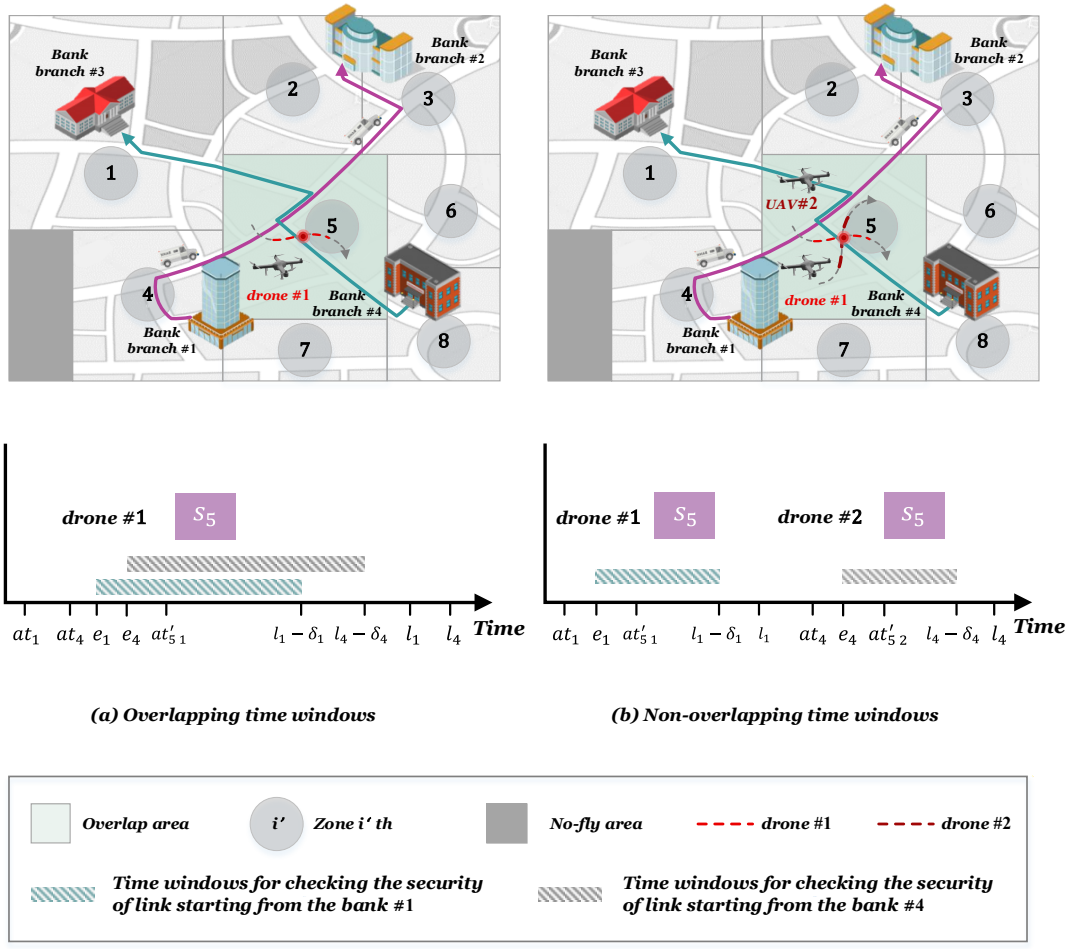

Fig. 5. The procedure of two ground links with common aerial zone center visited

Using a single drone to surveil a zone that spans two or more different links (as illustrated in Fig. 5 (a)) occurs when the sum of the parameters $z_{ij}^{i'}$ on the existing links is more significant than one, and their time windows ($[e_i, l_i - \delta_i]$) overlap. The sum of the $z_{ij}^{i'}$ parameter on the link for the network depicted in Fig. 5 is as per Fig. 6. The sum of $z_{ij}^{i'}$on links 4-3 and 1-2 for zone 5 is equal to 2, indicating that if their time windows overlap, a drone can be monitored simultaneously on two links of 4-3 and 1-2 in aerial zone 5. Otherwise, two different drones are used to surveil zone 5 for links 4-3 and 1-2.

$z_{ij}^{i'} =$

Scope centers (i') \ links (ij)	11	12	13	14	21	22	23	24	31	32	33	34	41	42	43	44	sum
1	0	0	1	0	0	0	1	0	1	1	0	1	0	0	1	0	1
2	0	1	0	0	1	0	1	1	0	1	0	0	0	1	0	0	1
3	0	1	0	0	1	0	1	1	0	1	0	0	0	1	0	0	1
4	0	1	1	1	1	0	0	0	1	0	0	0	1	0	0	0	1
5	0	1	0	0	1	0	0	1	0	1	0	1	0	1	1	0	2
6	0	0	0	0	0	0	0	0	0	0	0	0	0	0	0	0	0
7	0	0	0	1	0	0	0	0	0	0	0	0	1	0	0	0	0
8	0	0	0	1	0	0	0	1	0	0	0	1	1	1	1	0	1

Fig. 6. $z_{ij}^{i'}$ parameter and the overlap of surveillance of the aerial zone centers

Below are the constraints that apply this state to the problem. Constraints (3) and (4) define surveillance zones for links. Constraints (5) and (6) apply to drone time windows, in which a drone is permitted to visit the common zone only once if the time windows overlap.

$$\sum_{a=1}^{|A|}\sum_{k=1}^{|K|}\sum_{j=1}^{N}\sum_{i=0}^{N} x_{ijk}\, L_{ij}^{i'a}\, z_{ij}^{i'} \le \sum_{k=1}^{|K|}\sum_{j=1}^{N}\sum_{i=0}^{N} x_{ijk}\, z_{ij}^{i'} \quad \forall i' \in C \tag{3}$$

$$L_{ij}^{i'a} \le \sum_{j'=0}^{N'} y_{i'j'a} \quad \forall i,j \in C, \forall i' \in C, \forall a \in A \tag{4}$$

$$at_{i'a}^{'} \ge e_i\left(\sum_{k=1}^{|K|} x_{ijk}\, L_{ij}^{i'a}\, z_{ij}^{i'} - \left(1 - \sum_{k=1}^{|K|} x_{ijk}\, L_{ij}^{i'a}\, z_{ij}^{i'}\right) BigM\right) \quad \forall i,j \in C, \forall i' \in C, \forall a \in A \tag{5}$$

$$at_{i'a}^{'} \le (l_i - \delta_i)\left(\sum_{k=1}^{|K|} x_{ijk}\, L_{ij}^{i'a}\, z_{ij}^{i'} + \left(1 - \sum_{k=1}^{|K|} x_{ijk}\, L_{ij}^{i'a}\, z_{ij}^{i'}\right) BigM\right) \quad \forall i,j \in C, \forall i' \in C, \forall a \in A \tag{6}$$

where $at_{i'}^{'}$ denotes the arrival time to the aerial zone center i'. $L_{ij}^{i'a}$ indicates that if link ij is covered by drone a at zone i', it will equal 1. Otherwise, it will equal 0.

Indices, problem parameters, and variables are also listed below.

Nomenclature of mathematical formulation

Indices

i,j	Indices of banks and central treasury ($i,j \in C = \{0,1,2,...,N\}$)
i',j'	Indices of aerial zone centers ($i',j' \in \mathcal{C} = \{0,1,2,...,N'\}$)
k	Index of ground vehicles ($k \in K = \{1,2,...,\|K\|\}$)
a	Index of drones ($a \in A = \{1,2,...,\|A\|\}$)

Parameters

c_{ij}	Travel cost between customer i and customer j
$c'_{i'j'}$	Travel cost between area center i' and area center j'
γ	Cost per each transportation unit in each link
m_i	The demand of customer i
t_{ij}	Travel time between customer i and customer j
$t_{i'j'}$	Travel time between area center i' and area center j'
f_i	The time needed to service customer i
q_k	The capacity of ground vehicle k
r_k	Maximum allowed time of ground vehicle k
r'_a	Maximum allowed time of drone a
$z_{ij}^{i'}$	If the aerial zone center i' Covers link ij, it will equal 1. Otherwise, it will equal 0.
Δ_i	Maximum time interval for drone surveilling on aerial zone covering the outbound link of bank i
δ_i	The time gap between replanning and the time of leaving bank i
p_{ij}	Probability of robbery in link ij
τ_0	Minimum possible time for the ground vehicle to leave the depot
$\pi_{i'}$	The time required for controlling drones from aerial zone i'
$BigM$	A big number

Decision variables

x_{ijk}	The variable is set to 1 if the ground vehicle k travels from customer i to customer j
$y_{i'j'a}$	The variable is set to 1 if the drone a travels from the area center i' to area center j'
$L_{ij}^{i'a}$	If drone a visits aerial zone center i' To cover link ij, it will equal 1. Otherwise, it will equal 0.
$h_{ijk}^{i'a}$	Auxiliary variable for linearization of the proposed model
e_i	The minimum possible time required for drones to service the aerial zone covering the outbound link of bank i
l_i	Exit time of ground vehicle from bank i
at_i	Arrival time at customer i
$at_{i'a}$	Arrival time of drone a at area center i'
$w_{i'a}$	Waiting time of drone a at area center i'
D_{ij}^k	The load of ground vehicle k when travels from node i to node j
$\mathcal{P}_i^k$	Probability of no robber attack until reaching customer i by ground vehicle k
R_{ij}^k	The risk of ground vehicle k when travels from node i to node j

The objective function of the problem includes minimization of transportation cost (including costs of fuel, ground fleet driver, and drone battery charge) and cash transportation risk costs. The mathematical model of the proposed problem is indicated below.

$$f = in\begin{cases} \sum_{k=1}^{|K|}\sum_{j=0}^{N}\sum_{i=0}^{N} c_{ij}x_{ijk} + \sum_{a=1}^{|A|}\sum_{i'=0}^{N'}\sum_{j'=0}^{N'} c'_{i'j'}\, y_{i'j'a} + \\ \sum_{k=1}^{|K|}\sum_{j=0}^{N}\sum_{i=0}^{N} \gamma R_{ij}^{k} = \sum_{k=1}^{|K|}\sum_{j=0}^{N}\sum_{i=0}^{N} \gamma p_{ij}\mathcal{P}_{i}^{k}D_{ij}^{k} \end{cases} \quad (7)$$

s.t. (8)

$$\sum_{k=1}^{|K|}\sum_{j=1}^{N} x_{0jk} \le |K| \quad (9)$$

$$\sum_{\substack{j=0 \\ j\neq i}}^{N} x_{ijk} - \sum_{\substack{j=1 \\ j\neq i}}^{N} x_{jik} = 0 \qquad \forall i \in C, \forall k \in K \quad (10)$$

$$\sum_{\substack{j=0 \\ j\neq i}}^{N} x_{ijk} \le 1 \qquad \forall i \in C, \forall k \in K \quad (11)$$

$$\sum_{k=1}^{|K|}\sum_{\substack{i=1 \\ i\neq j}}^{N} x_{ijk} = 1 \qquad \forall j \in C\backslash\{0\} \quad (12)$$

$$at_i + f_i + t_{ij} - (1 - x_{ijk}) \times BigM \le at_j \qquad \forall i \in C\backslash\{0\}, \forall k \in \quad (13)$$

$$at_i + f_i + t_{ij} + (1 - x_{ijk}) \times BigM \ge at_j \qquad \forall i \in C\backslash\{0\}, \forall k \in K, \quad (14)$$

$$at_i + f_i + t_{i0} - (1 - x_{i0k}) \times BigM \le r_k \qquad \forall i \in C\backslash\{0\} \\ , \forall k \in K \quad (15)$$

$$\sum_{k=1}^{|K|}\sum_{\substack{i=1 \\ i\neq j}}^{N} D_{ji}^{k} - \sum_{k=1}^{|K|}\sum_{\substack{i=1 \\ i\neq j}}^{N} D_{ij}^{k} = m_i \qquad \forall i \in C\backslash\{0\} \quad (16)$$

$$D_{ij}^{k} \le x_{ijk}\, q_k \qquad \forall i,j \in C\,,\, i \neq j\,, \\ \forall k \in K \quad (17)$$

$$\sum_{a=1}^{|A|}\sum_{j'=1}^{N'} y_{i'j'a} \le |A| \qquad i' = 0 \quad (18)$$

$$\sum_{\substack{j'=0 \\ j'\neq i'}}^{N'} y_{i'j'a} - \sum_{\substack{j'=0 \\ j'\neq i'}}^{N'} y_{j'i'a} = 0 \qquad \forall i' \in \mathcal{C}, \forall a \in A \quad (19)$$

$$\sum_{\substack{j'=0 \\ j'\neq i'}}^{N'} y_{i'j'a} \le 1 \qquad \forall i' \in \mathcal{C}, \forall a \in A \quad (20)$$

$$y_{i'i'a} = 0 \qquad \forall i' \in \mathcal{C}, \forall a \in A \quad (21)$$

$$at'_{i'a} + t'_{i'j'} + \pi_{i'} + w_{i'a} - (1 - y_{i'j'a}) \times BigM \le at'_{j'a} \qquad \forall i' \neq j' \in \mathcal{C}, \forall j' \in \mathcal{C}\backslash \quad (22)$$

$$at'_{i'a} + t'_{i'j'} + \pi_{i'} + w_{i'a} + (1 - y_{i'j'a}) \times BigM \ge at'_{j'a} \qquad \forall i' \neq j' \in \mathcal{C}, \forall j' \in \quad (23)$$

$$at'_{i'a} + t'_{i'0} + \pi_{i'} + w_{i'a} - (1 - y_{i'j'a}) \times BigM - at'_{0a} \le r'_a \qquad \forall i' \in \mathcal{C}\backslash\{0\}, \forall a \in A \quad (24)$$

$$\sum_{a=1}^{|A|}\sum_{k=1}^{|K|}\sum_{j=1}^{N}\sum_{i=0}^{N} x_{ijk}\, L_{ij}^{i'a}\, z_{ij}^{i'} \le \sum_{k=1}^{|K|}\sum_{j=1}^{N}\sum_{i=0}^{N} x_{ijk}\, z_{ij}^{i'} \qquad \forall i' \in \mathcal{C} \qquad (25)$$

$$L_{ij}^{i'a} \le \sum_{j'=0}^{N'} y_{i'j'a} \qquad \forall i,j \in C, \forall i' \in \mathcal{C}, \forall a \in \quad (26)$$

$$l_i - \Delta_i = e_i \qquad \forall i \in C \qquad (27)$$

$$at_i + f_i = l_i \qquad \forall i \in C \backslash \{0\} \qquad (28)$$

$$at_0 \ge \tau_0 \qquad (29)$$

$$\sum_{a=1}^{|A|}\sum_{k=1}^{|K|} x_{ijk}\, L_{ij}^{i'a}\, z_{ij}^{i'} \le 1 \qquad \forall i \in C, \forall j \in C \backslash \{0\}, \quad (30)$$

$$at_{i'a}^{'} \ge e_i \left(\sum_{k=1}^{|K|} x_{ijk}\, L_{ij}^{i'a}\, z_{ij}^{i'} - \left(1 - \sum_{k=1}^{|K|} x_{ijk}\, L_{ij}^{i'a}\, z_{ij}^{i'}\right) BigM \right) \qquad \forall i,j \in C, \forall i' \in \mathcal{C}, \forall a \quad (31)$$

$$at_{i'a}^{'} \le (l_i - \delta_i) \left(\sum_{k=1}^{|K|} x_{ijk}\, L_{ij}^{i'a}\, z_{ij}^{i'} + \left(1 - \sum_{k=1}^{|K|} x_{ijk}\, L_{ij}^{i'a}\, z_{ij}^{i'}\right) BigM \right) \quad i \in C, \forall i' \in \mathcal{C}, \forall a \in A \qquad (32)$$

$$\mathcal{P}_i^k \ge (1 - p_{ji})\, \mathcal{P}_j^k x_{jik} \qquad j \ne i \in C, \forall k \in K \qquad (33)$$

$$\mathcal{P}_0^k = \sum_{j=0}^{N} x_{0jk} \qquad \forall k \in K \qquad (34)$$

$$x_{ijk}, L_{ij}^{i'a}, y_{i'j'a} \in \{0,1\}\ ,\ e_i, e_i, at_i, at_{i'a}^{'}, w_{i'a}, D_{ij}^k, \mathcal{P}_i^k \ge 0\ \ ,\ \ \forall i,j \in C\ ,\ \forall i',j' \in \mathcal{C}\ , \forall k \in K\ , \forall a \in A \qquad (35)$$

Equation (7) denotes the problem's objective function, which minimizes risk and transportation costs. Constraint (8) ensures that the central treasury receives a maximum number of $|K|$ ground vehicles. Constraints (9), (10), and (11) ensure that a single ground vehicle visits each bank exactly once. Constraints (12) and (13) determine the time required for ground vehicles to arrive at each bank branch. Constraint (14) relates to the maximum service time a ground vehicle may operate. Constraint (15) calculates the amount of cash transported by a ground vehicle at each link. Equation (16) limits the capacity of ground vehicles. Constraint (16) ensures that the central treasury receives the maximum number of $|A|$ drones. Constraint (18) regulates the drone's entry and exit from each aerial zone center. Constraint (19) ensures that each drone does not visit or visit each aerial zone center only once. Constraint (20) prohibits drone movement from one aerial zone center to the same aerial zone center. Constraints (21) and (22) determine the drone's arrival time at each aerial zone center. Constraint (23) limits the drone's maximum flight time. Constraints (24) and (25) apply to the movement of drones and ground vehicles. In other words, this constraint ensures that drones fly over ground vehicle routes in aerial zone centers. Constraints (26) to (31) control the link based on the temporal relationship between drone and ground vehicle movement. At each link, constraints (32) and (33) calculate the probability of no theft from ground vehicles.

3.2. Risk minimization

This section discusses the risk-reduction strategies considered in this study. Risks associated with intentional disruption of cash transportation are minimized in two stages. Prior to the start of transportation, the planning phase assesses and estimates the risk of cash robbery along transportation routes. After planning and establishing cash transportation and drone surveillance routes, drones assess the risk associated with each link before ground vehicles begin moving through each link. As a result, Section 3.2.1 proposes a formula for calculating risk based on influential factors, while Section 3.2.2 discusses the properties of surveillance drones and assessment methods.

3.2.1. Risk estimation

The risk is proportional to the length of the link, the probability of robbery in each link, and the load transported by ground vehicle. As the link's length increases, more dangers confront the ground vehicle. The load of a ground vehicle also affects the severity of an accident. Assume that the ground vehicle contains additional cash at the time of the robbery. As a result, the risk is calculated using Equation (36).

$$R_{ij}^{k} = p_{ij}\mathcal{P}_{i}^{k}L_{ij}^{k} \tag{36}$$

3.2.2. Risk assessment by drones

Following the identification of ground vehicles and drones, drones assess and predict potential risks along transportation routes. Before ground vehicles pass through a link, drones fly over the aerial zone that covers the ground routes, assessing their security. They are purely surveillance devices, and in the event of observing a suspected case, they alert the security control room (SCR) to reroute the ground vehicle. Additionally, drones can identify and track robbers, ground vehicles (their movement and type), weapons, and explosive devices (Yaacoub and Salman, 2020). Furthermore, because drones are more maneuverable than fixed cameras, they can detect hidden suspected targets in public spaces. Drones can also identify suspects based on their age, size, and face when they are out in public. Moreover, some drones employ shape detection algorithms to identify weapons (Karim et al., 2017). Furthermore, they estimate individuals' weights and detect weapons and smuggled materials using shaking sensors (Lee et al., 2019).

The drones in the proposed problem are also equipped with a camera for image capture and video recording and two control and processing units for overall operation control. One unit detects suspicious materials, including weapons; sensors and cameras automate this process. The other unit is concerned with the ground vehicle's movement.

3.3. The dynamic procedure of tackling intentional disruption

As previously stated, an integrated routing solution and ground and aerial vehicle surveillance are created first, as illustrated in Fig. 1. Afterward, the network is implemented with the integrated

ground vehicle and drone solution until the drones detect a threat caused by intentional disruption at the time t_r in links. The system's information is updated in this case, and the most dangerous ink is removed from the transportation network. As a result, the mathematical model's sets, variables, and parameters are optimized in response to the following changes. Additionally, Section 5.5 discusses the details of removing the problem's most dangerous link.

- The ground customer set changes from $C = \{0,1,2,...,N\}$ to $C_D = \{0,...,N_D\}$. Thus, the C_D set contains customers who have not received the service. In other words, these customers are removed from the set of all customers (C).
- The set of aerial zones remains constant.
- The $t_r + \varepsilon$ parameter is defined as the initial encounter with risk in risk zones (the risk zone is the zone where the robber is detected by the drone)
- It is prohibited for ground vehicle k to enter links that pass through the risk zone i' at shorter times. Constraint (37) is added to the model to apply this assumption.

$$at_{i'a}' > t_r \qquad \forall i' \in C, \forall a \in A \qquad (37)$$

- The variable sx_{ijk} and $y_{i'j'a}$ are set based on the transportation routes (x_{ijk} and $y_{i'j'a}$ will be equal to 1 for passed links or links passed after time t_r).
- Ground vehicle capacity for vehicles departing the depot will be increased to match their loads.
- The arrival time of ground vehicles (at_i) and drones ($at_{i'a}'$) is also affected by previously established ground and aerial links.
- Given the time required for drones to visit zones under new conditions when a threat is detected in those zones, the ground vehicle waits in bank locations for a period of time. As a result, variable w_i is defined to represent the ground vehicle's waiting time, and constraints (12) and (13) are replaced by constraints (38) and (39), respectively.

$$at_i + f_i + t_{ij} + w_i - (1 - x_{ijk}) \times BigM \leq at_j \qquad \forall i \in C\backslash\{0\}, \forall k \in K, \forall j \neq i \in C \qquad (38)$$

$$at_i + f_i + t_{ij} + w_i + (1 - x_{ijk}) \times BigM \geq at_j \qquad \forall i \in C\backslash\{0\}, \forall k \in K, \forall j \neq i \in C \qquad (39)$$

After updating the information, the system can reroute the vehicles based on the new risk conditions in the ground links, from the time the danger (robber) is identified to the time the vehicle leaves the bank (l_i) and provide a new, lower-risk solution to be implemented. To be more precise about the time window, Fig. 7 illustrates the relationship between critical time parameters based on the assumption that drone 1 surveils the link ij in the aerial zone center i' and detects a robber in this link.

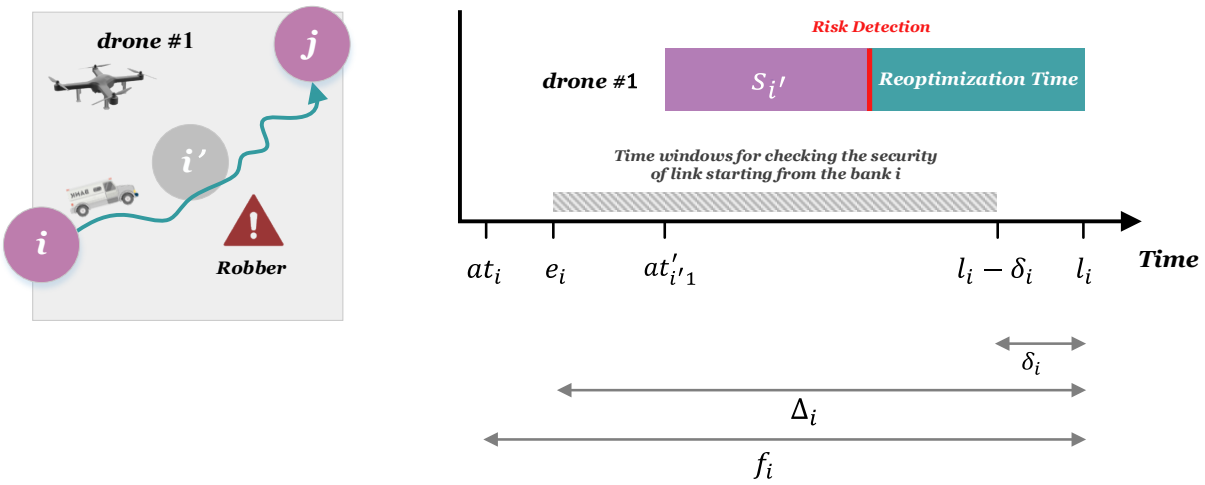

Fig. 7. The order of the problems' critical time parameters

4. Solution algorithm

The D-SALNS algorithm, which combines ALNS and SA algorithms, is proposed in this section for solving large-scale problems. ALNS is a modified version of the LNS problem, one of the most successful algorithms in this field (Mohri et al., 2020). This algorithm begins by generating an initial solution. After that, removal and insertion operators will make some modifications to the initial solution. For each iteration, a single operator is chosen based on its weight. The weight of the removal and insertion operators is calculated for each iteration based on their performance. The roulette wheel then selects one algorithm for removal and one for insertion. Additionally, the SA algorithm is used to accept and reject new solutions. The D-SALNS pseudocode algorithm is denoted by Algorithm 1.

Algorithm 1: D-SALNS

Input:

Parameters of IRS instances

Parameters of ALNS

Parameters of SA

Output: A optimum solution

Construct an initial solution S_0;
$S, S_{best} \leftarrow S_0$
Initialize weights of removal and insertion operators;
$iter \leftarrow 1$
While $iter < MaxIt$
    select a pair of removal and insertion operators;
    Apply the removal operator to S;
    Apply the insertion operator to S and construct S_{temp};
    Make S_{temp} infeasible;
    Apply local search on S_{temp}^{drone};
    if $T_{temp} < T_{best}$
        $S, S_{best} \leftarrow S_{temp}$
    else
        $S \leftarrow S_{temp}$
    end
update the weights and scores of removal and insertion operators;
$iter \leftarrow iter + 1$
end While

4.1. Representation

Coding the solution presentation is a step in the meta-heuristic algorithm optimization process. The solution to this problem is presented using ground vehicles and drones and the connection between the two fleets. Fig. 8 depicts the solution representation in the proposed algorithm.

The Ground Vehicle Solution and Aerial Vehicle Solution cells in Fig. 8 illustrate the order of point passes on the ground and aerial routes, respectively. The Ground Vehicle and Aerial Vehicle cells also display the number of nodes traversed by vehicles along each route. Furthermore, the Ground Points 2 Aerial Point cell shows all zones that the drone must survey and control to reach that point. For example, the first row of this representation contains the numbers 3, 2, 5, and 4, indicating that the drone must monitor and control zones 3, 2, 5, and 4 in order for the ground vehicle to reach customer 1. The Ground Points 2 Aerial Routes cell is identical to the previous one, except that it displays the number of drones that have passed through the assessed zones. In other words, drones 1, 3, 1, and 3 are used to visit zones 3, 2, 5, and 4 in the first row, respectively.

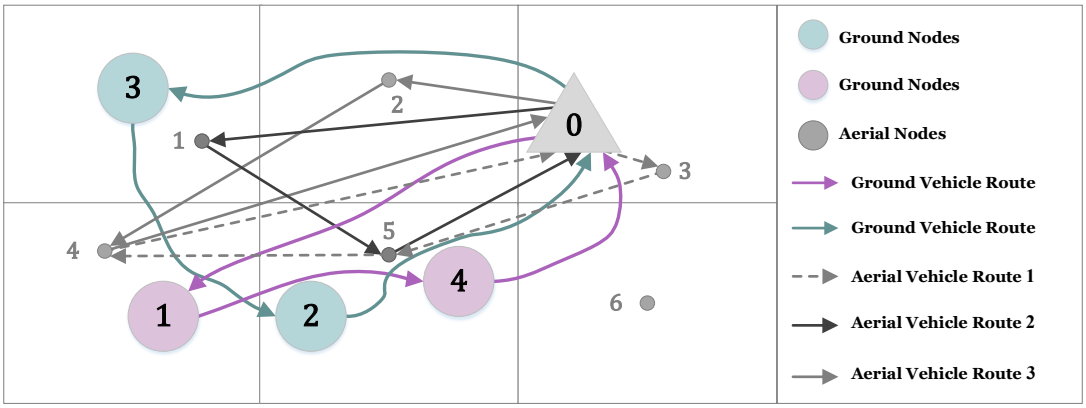

Ground Vehicle Solution :

3	2	1	4

Ground Vehicle :

2	2

Aerial Vehicle Solution :

3	5	4	1	5	2	4

Aerial Vehicle :

3	2	2

Ground Points 2 Aerial Point :

3	2	5	4
1	4	5	0
3	2	1	0
4	5	0	0

Ground Points 2 Aerial Routes :

1	3	1	3
2	1	2	0
1	3	2	0
1	2	0	0

Fig. 8. Representation of D-SALNS

4.2. Initial solution

The initial solution at static state is generated randomly. In the dynamic case, the initial solution is greedy, as one of the primary objectives is to minimize optimization time.

4.3. Removal operators

The primary goal of removal operators is to eliminate one or more points from the solution. Eleven removal operators are used in this algorithm to remove the points, as listed below.

Random Removal (RR): One or two points are randomly selected from the ground vehicle solution and removed in this operator.

Worst Cost Removal in the ground vehicles (WCR): This operator eliminates the ground vehicle solution's most expensive points. The highest cost is calculated as $j^* = \text{argmax}_{j \in N}\{|F_{ij} + F_{jk}|\}$. As a result, F_{ij} equals the trip cost and risk associated with link ij.

Worst Total Cost Removal in the ground and aerial vehicles (WTCR): This operator eliminates the ground vehicle solution point and the associated costs from the drone solutions. The highest total cost is calculated as $j^* = \text{argmax}_{j \in N}$

$\{|F_{ij} + F_{jk}| + \sum L_{ij}^{j'a}(F'_{i'j'} + F'_{j'k'})\}$. Accordingly, F_{ij} and $F'_{i'j'}$ are the trip cost and risk in link ij, and the drone flight cost in link $i'j'$, respectively.

Worst Time Removal in the ground vehicles (WTR): This operator eliminates the most time-consuming aspect of the ground vehicle solution. The worst possible time is calculated as $j^* = \text{argmax}_{j \in N}\{|t_{ij} + t_{jk}|\}$.

Worst Total Time Removal in the aerial and ground vehicles (WTTR): This operator eliminates the most time-consuming ground vehicle solution point from the corresponding drone solution, as well as the associated costs. The worst total time is calculated using the formula $j^* = \text{argmax}_{j \in N}\{|t_{ij} + t_{jk}| + \sum L_{ij}^{j'a}(t'_{i'j'} + t'_{i'j'})\}$.

Shaw removal (SR): This operator was first introduced by Shaw (1998). This operator seeks to eliminate a group of customers who are somehow connected. Initially, this algorithm randomly selects one point and adds it to the removal list. Following that, one [point is selected and added to the list using the $j^* = \text{argmin}_{j \in N}$ $\{\varphi_1 d_{ij} + \varphi_2|at_i - at_j| + \varphi_3 l_{ij} + \varphi_4|m_i - m_j|\}$ formula of the next point. In this formula, the weights φ_1, φ_2, φ_3, and φ_4 are considered, and their sum equals 1. If the second point (i) is on the same route as the first point (j), and if $l_{ij} = -1$ is on a different route, $l_{ij} = 1$ (weight of all four factors are considered identical).

Proximity-based Removal (PR): This operator chooses two points with the shortest distance between them at random. Indeed, this operator is a special case of the Shaw operator, where $\varphi_1 = 1$ and $\varphi_2 = \varphi_3 = \varphi_4 = 0$.

Time-Based Removal (TR): This operator is a special state of the Shaw operator, where $\varphi_2 = 1$ and $\varphi_1 = \varphi_3 = \varphi_4 = 0$.

Demand-based Removal (DR): This operator is a special state of the Shaw operator, in which $\varphi_4 = 1$ and $\varphi_1 = \varphi_2 = \varphi_3 = 0$.

Historical knowledge node removal (HR): At each repeat, this operator records the cost of a point as $F_j = F_{ij} + F_{jk}$. The value of F_j^* is equal to the minimum value of F_j, which is updated at each repeat. This operator chooses a point whose cost is the most significant deviation from the best cost point. In other words, the point calculated using the formula $j^* = \text{argmax}_{j \in N}\{F_j - F_j^*\}$ is selected (Demir et al., 2012).

Neighborhood Removal (NR): This operator selects one operator at random and then removes one or two relevant points (before or after that point).

4.4. Insertion operators

This operator attempts to reintroduce the removed point into the solution using various rules. Three insertion operators are proposed for this purpose, as listed below.

Greedy insertion (GI): This operator positions each point optimally in terms of cost. If the cost of point j is calculated as $F_j = F_{ij} + F_{jk} - F_{ik}$, the point selected by this operator will be $j^* = \text{argmin}_{j \in N}\{|F_j|\}$.

Greedy insertion with noise function (GIN): This operator is a developed version of GI that utilizes one degree of freedom to determine the optimal position for this point. This degree of freedom is obtained by setting the rank of point i to $NewRank = ActualRank + \overline{r}\mu\epsilon$. $\overline{r}$ is the worst rank, and μ is the noise parameter used to generate distributions in the generated solutions and is set to 0.1. ϵ is a random number between $[-1, 1]$.

Residual Time Insertion (RTI): This operator is determined by the residual time on each route. In other words, routes with a shorter residual time after customer addition are more likely to be accepted than routes with a longer residual time. The formula used in this operator is similar to the one proposed by Guo et al. (2021) for Modified Regret k Insertion (MRkI). Thus, the points obtained by $j^* = \text{argmin}_{j \in N}\{\varphi_1(F_{ij} + F_{jk} - F_{ik}) + \varphi_2(u - u)\}$ are regarded as the operator's selected points. In this formula, φ_1 and φ_2 are the cost and time factor weights, respectively, and their sum equals 1. u and u' also represent the value of residual time along each route prior to and following the addition of point.

4.5. Adaptive layer

The ALNS algorithm applies one removal and one insertion operator to the solution via the roulette wheel at each iteration. Setting the weights of removal and insertion operators is a component of an adaptive search mechanism. First, the weights of all operators are assumed to be equal. Following that, the search is divided into ρ sections to calculate weights. After each section, the weight assigned to each operator is determined by the score earned. This paper used the weighting approach outlined in Kuhn et al. (2021).

After applying the σ_1, σ_2, σ_3, and σ_4 parameters, the score of each operator increases. According to Table 2, if the solution is generated by the objective function of the best solution (T_{best}) is accepted, the score of the removal and insertion operators increases by σ_1 units. Otherwise, the noise is carried out. The incumbent solution value of the objective function (T_{inc}) is multiplied by γ in this case. Suppose that the objective function's temporary solution value (T_{temp}) is greater than $T_{inc}\,\gamma$; the temporary solution is then removed, and the scores of the removal and insertion operators are increased by σ_4 units. Otherwise, the temporary solution will be accepted, and the problem will be examined in two instances. Suppose that the objective function's temporary solution value is greater or less than its incumbent solution value; in this case, the scores of the removal and insertion operators increase by σ_2 and σ_3 units, respectively. It is worth noting that the $\sigma_4 < \sigma_3 < \sigma_2 < \sigma_1$ equation is always true when four weight parameters are used.

Table 2. States of temporary solution in the proposed algorithm

State	Consequence	Weight parameter
1) $T_{temp} < T_{best}$	best and incumbent solution are updated	σ_1
2) $T_{temp} < T_{inc}\,\gamma$	incumbent solution is updated	
2a)	$T_{temp} < T_{inc}$	σ_2
2b)	$T_{temp} \geq T_{inc}$	σ_3
3) else	temporary solution is rejected	σ_4

The value of γ is a random value within the range $[\underline{\gamma},\overline{\gamma}]$, such that $\underline{\gamma} \leq 1$ and $\overline{\gamma} \geq 1$. Additionally, $\underline{\gamma}$ and $\overline{\gamma}$ are calculated as$\underline{\gamma} = 1 - \underline{\gamma}_{best} - \underline{\gamma}_{inc}$ and $\overline{\gamma} = 1 + \overline{\gamma}_{best} + \overline{\gamma}_{inc}$. Furthermore, $\overline{\gamma}_{inc}$ parameters, as well as $\underline{\gamma}_{best}$ and $\overline{\gamma}_{best}$ performance are updated after a specified number of iterations in the algorithm without regard for the order in which incumbent and best solutions are found (ψ). The relevant parameters' values are reset when a new incumbent or optimal solution is identified.

The weight of operators i (φ_i) is calculated according to Equation (40):

$$\varphi_i = (1 - \tau_A)\varphi_i + \tau_A \frac{\pi_i}{\xi_i} \tag{40}$$

where π_i and ξ_i denote the scores obtained by operator i and frequency of utilizing operator i, respectively. Also, operator τ_A is the reaction factor.

4.6. Neighborhood Search

Neighborhood search is implemented on drone routes during each internal iteration of the algorithm. Neighborhood search is a one-point type. This algorithm eliminates one point from the drone solutions and replaces it with a more cost-effective route.

4.7. Feasibility

Constraints and feasibility of the inserted point are evaluated during the point insertion step. The solution is examined using the operator's rules if the inserted point is feasible. However, the infeasible solution may also be generated in response to the problem's complexity. When a point is inserted into a solution, the time windows of all subsequent points change in addition to the inserted point. As a result, the drone links that were within their time windows prior to the insertion of the new point may change, and the solution may become unfeasible. Thus, a feasibility operator is defined in the algorithm after the removal and insertion operators to identify infeasible links and make them feasible by changing the drone solution's links.

4.8. Simulated annealing

SA is used in this study to accept or reject generated solutions s' that are close to the initial solution. If the solution objective function $s^{'}$ is superior to the best value, it is accepted. Otherwise, the probability of $exp\left[\left(f\left(s^{'}\right)-f(s)\right)/\theta\right]$ is the current temperature in this formula. First, the temperature is set to θ_0 and is reduced by multiplication at a rate of μ at each iteration.

5. Analysis of results

This section evaluates the problem and the proposed algorithm in stages. Initially, the IRS is compared to two other scenarios to determine its performance. Following that, the Taguchi method is used to set the D-SALNS algorithm's parameter. The proposed algorithm is then compared to CPLEX optimization software using the obtained parameters. After evaluating the D-SALNS algorithm's quality on a small scale, its performance on a large scale is also evaluated. The results of this algorithm are compared to those of the ALNS algorithm for this purpose.

5.1. Analyzing different scenarios of the problem

Three scenarios involving drone surveillance of cash transporter vehicles are examined in this section. Afterward, the three parameters are compared to one another, and the benefits and drawbacks of each are examined.

5.1.1. Scenario 1: identical ground vehicles and drones' routes

In this scenario, the drone follows the route of the ground vehicle precisely and surveils its movement. In other words, to ensure the ground vehicle's security, drones begin moving ahead of the ground vehicle and surveil its route. As a result, the routes taken by ground vehicles and drones are identical.

5.1.2. Scenario 2: Non-integrated ground vehicle and drones' routes

In this scenario, the problem is optimized first without taking drones into account, and then drones are assigned to routes based on the proposed problem. In other words, this scenario is divided into two distinct phases. The first phase involves determining the routes of ground vehicles, and the second phase involves allocating surveillance drones to the routes of ground vehicles.

5.1.3. Scenario 3 (IRS): Integrated ground vehicle and drones' routes

This approach integrates and optimizes both ground vehicle and drone routes concurrently.

5.1.4. Comparison of proposed scenarios

This section examines ten small-scale examples to determine the performance of each scenario. It is worth noting that these three scenarios affect only transportation costs and not risk-related costs.

Thus, transportation costs are used as the objective function for comparing the three scenarios. Table 3 summarizes the results obtained by resolving the problem and resolving time.

Table 3. The results obtained by three scenarios at small-scale problems

No.	NB	NZ	MNGV	MND	Total Cost			Total Time (s)			Active drones		
					S1	S2	S3	S1	S2	S3	S1	S2	S3
1	3	3	2	2	-	-	39.70	-	-	1.40	-	-	2
2	3	4	2	3	-	-	52.37	-	-	635.08	-	-	3
3	4	4	2	3	-	-	65.06	-	-	108.82	-	-	3
4	5	4	2	4	60.42	-	37.45	0.48	-	322.95	4	-	3
5	5	4	2	4	61.72	-	41.57	0.11	-	680.11	4	-	3
6	5	5	2	4	30.86	29.83	27.94	0.25	2.69	2299.50	4	4	2
7	6	4	2	4	39.44	26.06	22.38	0.20	0.09	4253.70	3	3	3
8	6	4	2	4	103.08	81.74	75.56	0.65	2.50	1260.86	4	3	3
9	4	6	2	4	78.88	-	69.32	4.75	-	1852.60	4	-	4
10	6	6	2	3	-	25.80	24.10	-	2.98	6652.40	-	3	2

NB: Number of Banks, NZ: Number of Zones, MNGV: Maximum number of ground vehicles, MND: Maximum number of drones, S1: Scenario 1, S2: Scenario 2, S3: Scenario 3.

According to the results of problems designed using the three scenarios, scenario 3 performs the best in terms of solution generation because it can calculate the solution at the lowest cost. However, while the solutions obtained through scenarios 2 and 3 may be identical in some cases, this is not always the case. Additionally, the second scenario may generate a workable solution to some issues. In other words, given the limited number of available drones and their maximum flight time, surveillance drones may not be assigned to the ground vehicle routes identified in the first phase. Scenario 3 addresses this issue.

Furthermore, Scenario 1 takes less time to solve than the other two scenarios. However, the costs associated with this scenario are higher than those associated with the other two scenarios, owing to the absence of concurrent surveillance on common zones. Moreover, this scenario may be incapable of producing feasible generation.

Example 8 from Table 3 is analyzed schematically to help visualize the three scenarios. This example induces six banks and one depot, which are distributed across four aerial zones. Additionally, three scenarios are provided to optimize this issue.

Scenario 1: Fig. 9 illustrates the results of problem optimization using this scenario. This solution's objective function value equals 103.08. This problem took 0/65 s to solve.

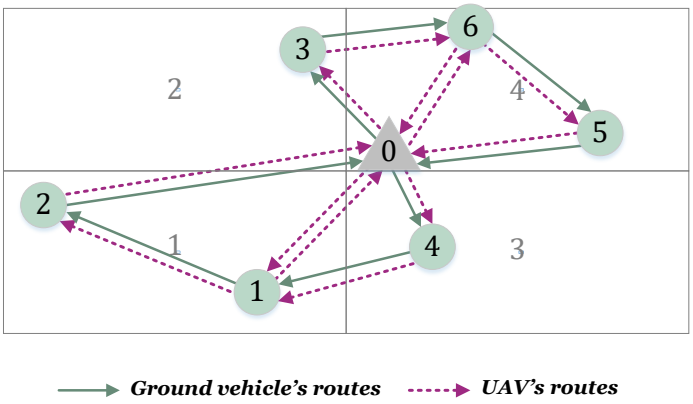

Fig. 9. The optimized solution obtained by scenario 1

Scenario 2: Fig. 10 illustrates the results of problem optimization using this scenario. This solution's objective function value equals 81.74. This problem took 2.5 s to solve.

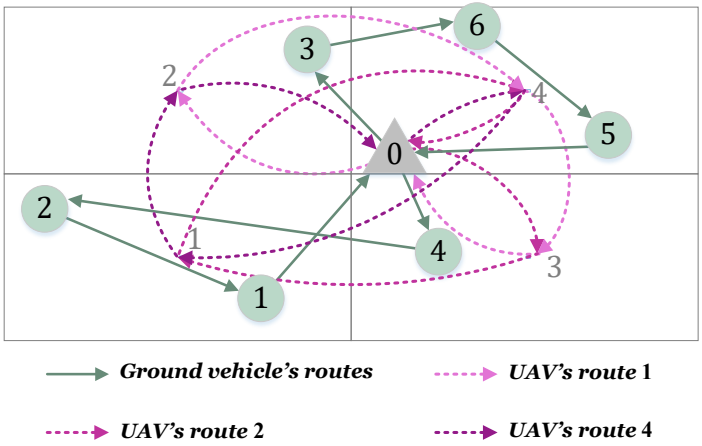

Fig. 10. The optimized solution obtained by scenario 2

Scenario 3: Fig. 11 illustrates the results of problem optimization using this scenario. This solution's objective function value equals 75.56. This problem took 1260.86 s to solve.

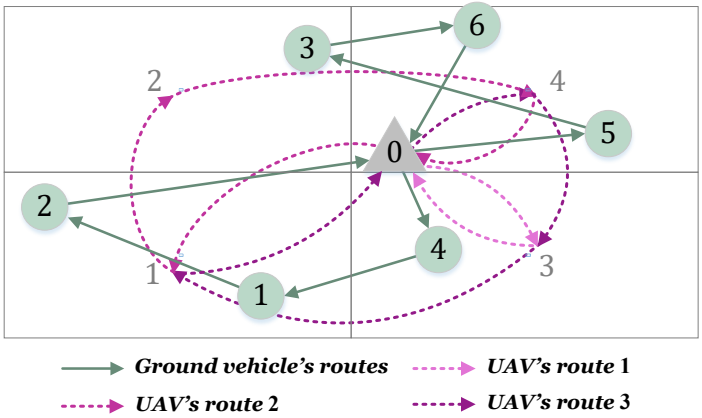

Fig. 11. The optimized solution obtained by scenario 3

5.2. Parameter setting

Parameter setting is used to optimize the algorithm's performance, avoid early convergence, and increase diversity in space search. In this study, the Taguchi and Wu (1980) method is used to set the parameters. The levels considered for algorithm parameters and the optimization levels obtained are listed in Table 4. According to (Goeke and Schneider, 2015, Yu et al., 2021), the initial temperature is selected such that a solution with an objective function 50% worse than the initial solution has a 50% probability of acceptance.

Table 4. Parameter adjustment of the D-SALNS algorithm

Parameters	Description	Level 1	Level 2	Level 3	Optimum level
$MaxIt$	Maximum number of iteration	1000	2000	3000	3000
ρ	Segment size	10	20	30	20
τ_A	Reaction factor	0.1	0.2	0.3	0.3
σ_1	Best score	9	10	11	11
σ_2	Improvement score	6	7	8	8
σ_3	Improvement score	3	4	5	5
σ_4	Worst score	0	1	2	0
γ	Realization of a random variable	0.1	0.2	0.3	0.1
ψ	Number of iteration without improvement	200	300	400	200
μ	Cooling rate	0.90	0.95	0.99	0.90

5.3. Small-scale analysis

In order to assess the proposed algorithm, the performance of the algorithm at a small scale is assessed by BARON solver of GAMS commercial software. For this purpose, five problems of small-size are designed and solved by the D-SALNS algorithm and BARON. Then, the size of problems is increased until the BARON solver cannot solve the problem at a reasonable time. Table 5 indicates the results obtained by comparison.

Table 5. Comparison of D-SALNS and BARON in small size problems

NO.	Number of ground point ($\|N\|$)	Number of aerial point ($\|N'\|$)	Objective			CPU Time (sec)		
			D-SALNS	BARON	Dev.	D-SALNS	BARON	Dev.
1	3	4	68.14	68.14	0.00	74.84	63.86	0.17
2	3	4	88.22	88.22	0.00	48.05	526.84	-0.91
3	4	4	89.87	89.87	0.00	35.40	79.83	-0.56
4	5	4	81.26	81.26	0.00	181.60	970.19	-0.81
5	5	4	99.10	99.10	0.00	167.17	2801.30	-0.94
6	6	4	106.76	-	-	121.13	-	-

According to Table 5, the D-SALNS algorithm obtains solutions equal to BARON when the size is small, indicating the algorithm's favorable quality. Additionally, BARON is incapable of solving problems of relatively small size in a reasonable amount of time. In other words, if a problem contains six ground points, four aerial points, or more, the software will be unable to solve it.

5.4. Large−scale analysis

The proposed algorithm is compared to the ALNS algorithm for large-scale problems that cannot be solved in a reasonable amount of time using the BARON solver included with GAMS software (this algorithm is similar to the D-SALNS algorithm expect that the added SA and neighborhood search operator are removed). Two algorithms are used to optimize 20 problems of varying sizes for this purpose. Table 6 summarizes the findings of this comparison.

Table 6. Comparison of D-SALNS and ALNS algorithms in large-scale problems

No.	Number of ground point ($\|N\|$)	Number of aerial point ($\|N'\|$)	Total cost			CPU Time (sec)		
			D-SALNS	ALNS	Dev.	D-SALNS	ALNS	Dev.
1	25	15	847.38	890.27	-0.05	2777.99	2684.34	0.03
2	25	20	822.18	852.26	-0.04	2766.07	3879.45	-0.40
3	25	25	813.09	880.78	-0.08	2535.53	3153.65	-0.24
4	25	25	1668.65	1883.65	-0.13	1564.24	2262.62	-0.45
5	25	30	822.73	879.07	-0.06	3954.47	5483.45	-0.39
6	25	35	808.89	823.65	-0.02	1539.04	1007.73	0.35
7	50	40	1557.83	1805.39	-0.14	11025.83	15539.68	-0.41
8	50	45	1645.10	2007.53	-0.18	15757.87	9652.47	0.39
9	50	50	1442.83	1771.68	-0.19	14705.41	14259.00	0.03
10	50	55	1566.34	1733.69	-0.10	17344.22	18670.97	-0.08
11	50	60	1599.48	1695.36	-0.06	9516.74	19458.96	-1.04
12	75	15	2284.17	2484.20	-0.08	8742.83	6904.13	0.21
13	75	20	2177.17	2254.82	-0.03	10738.07	16762.49	-0.56
14	75	25	2286.33	2463.89	-0.07	16221.47	25106.98	-0.55
15	75	30	2073.06	2437.54	-0.15	14524.22	10645.51	0.27
16	75	35	2257.46	2561.77	-0.12	7525.84	14035.94	-0.87
17	100	15	2392.81	2603.53	-0.08	4577.99	5436.22	-0.19
18	100	20	2577.95	2729.33	-0.06	5506.01	8108.71	-0.47
19	100	25	2563.53	2726.69	-0.06	8196.96	12022.24	-0.47
20	100	30	2475.59	2740.03	-0.10	12647.72	24558.17	-0.94
21	100	35	2453.85	3126.81	-0.22	26613.23	12747.50	0.52
Avg.					-0.11			-0.25

According to Table 6, the D-SALNS algorithm's objective function is lower than the ALNS algorithm's objective function in all problems. The D-SALNS algorithm is faster on average than the ALNS algorithm in solving time. As a result, it can be concluded that the modifications made to the ALNS algorithm result in time savings and improved solution quality. Fig. 12 illustrates the time and cost of solving in the D-SALNS and ALNS algorithms.

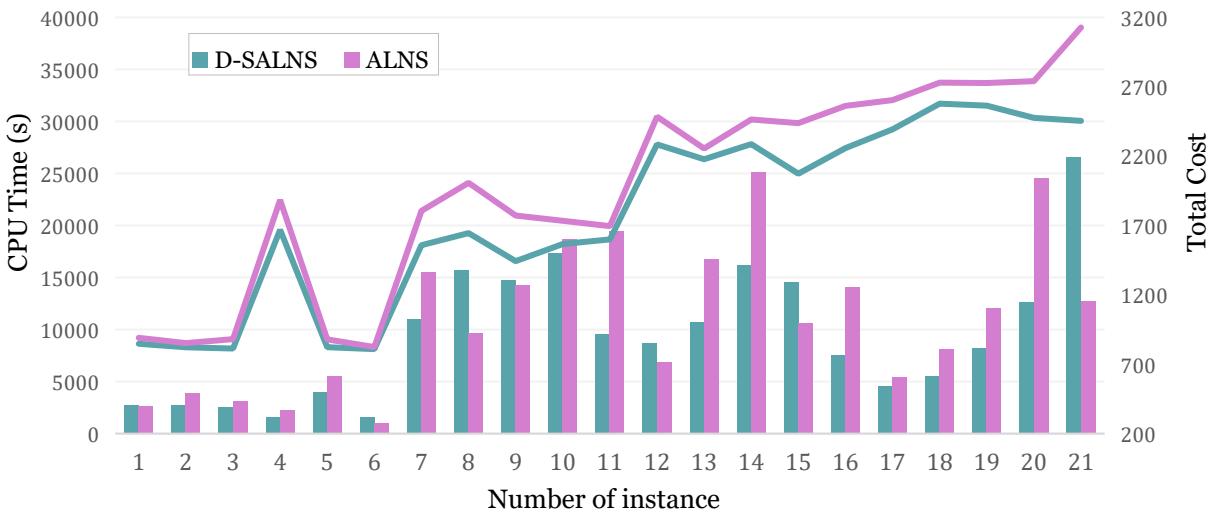

Fig. 12. Comparison between the objective function and solving time in D-SALNS and ALNS algorithms

Additionally, the improvement of solutions in D-SALNS and ALNS algorithms was compared for various problems. To this end, Fig. 12 indicates the value of the objective function in iterations of the algorithm until the value of the objective function is nearly constant and does not change.

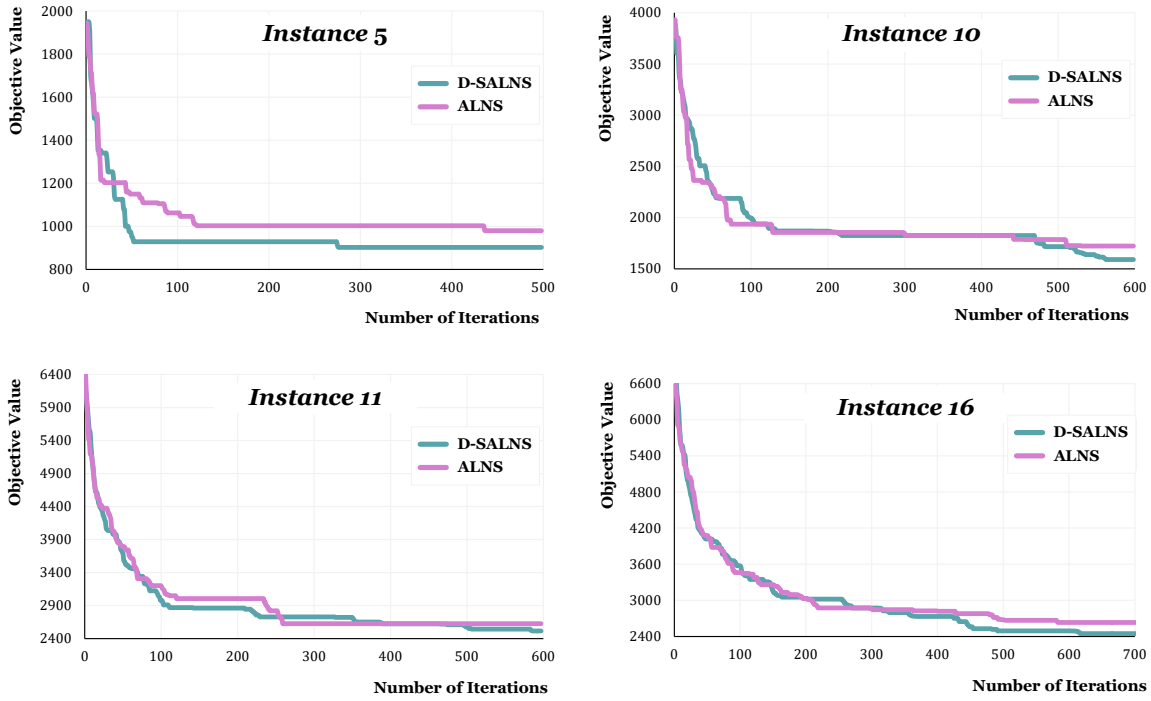

Fig. 13. Improvement trend of solutions generated by D-SALNS and ALNS algorithms

According to Fig. 13, the solutions generated by D-SALNS are more reducible than those generated by ALNS. Moreover, the number of solution improvement times in D-SALNS is greater than that in ALNS.

5.5. Problem analysis at the dynamic state

A problem from Section 5.4 (instance 4 in Table 6) is chosen to study and compare the problem statically and dynamically. The solution with the lowest cost, as defined in Section 5.4, is considered to be the chosen solution. Subsequently, it is assumed that the drones will detect an intentional disruption (attack) in a randomly selected link in the chosen solution. Finally, the problem is dynamically reoptimized by modifying the problem parameters. In static and dynamic states, the objective functions are 1668.65 and 2002.78, respectively. This cost includes ground and air travel, as well as risk.

Static and dynamic travel costs are 692.79 and 772.53, respectively, indicating travel costs increase during re-optimization. Without online monitoring of the drones, all valuable goods contained within the ground vehicle would be stolen, increasing the risk cost from 975.86 to 1478.14. However, monitoring drones and tracking their routes online reduced the risk cost from 1478.14 to 1230.25. Therefore, given the potential for life-threatening and irreversible consequences of striking the ground fleet, even if the cost of employing the drone exceeds the value of the stolen valuable goods, the use of drones may be justified for security reasons. Fig. 14 depicts the solution to the problem in a static state.

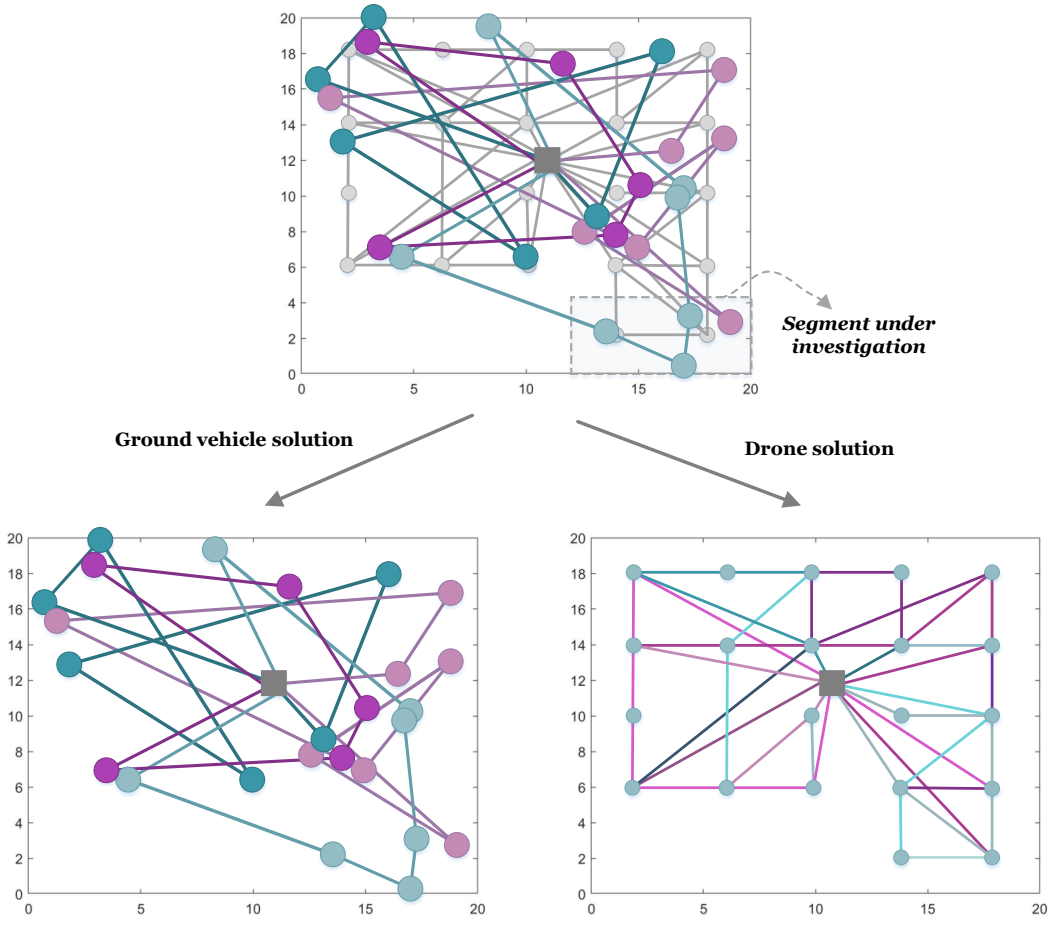

Fig. 14. Problem solution at a static state

A small segment of the problem is separated according to Fig. 15, and the changed parameters in this section are listed in Table 7 to illustrate the dynamic solution to the problem in greater detail. According to Fig. 15, the robber waits in ambush in zone 21 and link 17-24 and is identified by drone 2 at 27.38 in aerial link 16-21. Following that, replanning is performed by removing the risk source from the previously used solution and re-establishing security in zone 21 and its connections.

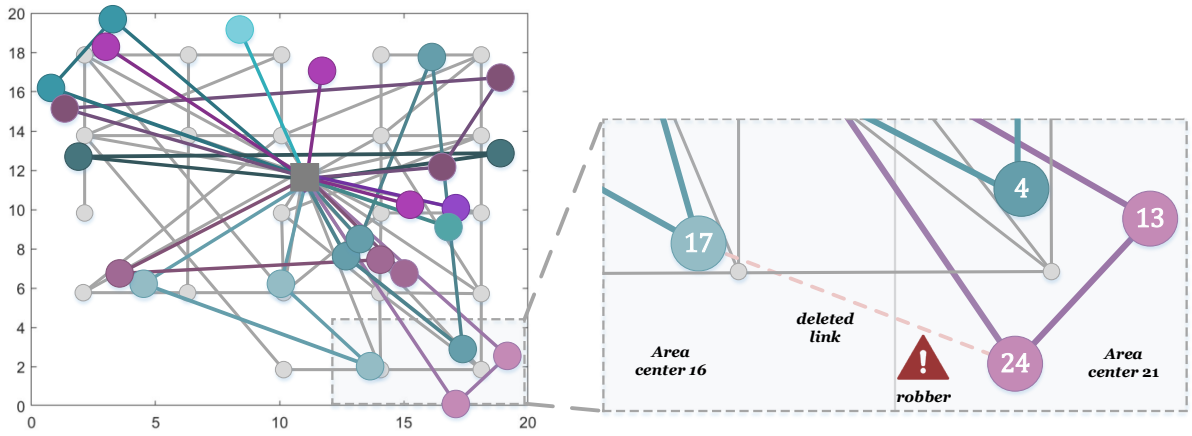

Dynamic solution **Segment under investigation**

Fig. 15. Problem solution at the dynamic state

Table 7. Value of some variables at static and dynamic states

variables	Value		variables	Value	
	static mode	dynamic mode		static mode	dynamic mode
x_{17-24}^{3}	1	0	t_r	-	27.38
x_{13-24}^{11}	0	1	$t_r+\varepsilon$	-	39.38
x_{24-0}^{11}	0	1	e_{24}	26.64	58.89
$y_{16-21\ 2}$	1	1	$l_{24}-\delta_{24}$	31.964	63.89
$y_{17-21\ 11}$	0	1	$at_{21}{}'_{11}$	-	62.11

According to Fig. 15 and Table 7, the static solution excludes ground link 17-24 due to the robber waiting to attack in zone 21. As a result, x_{17-24}^{2} is equal to 1 and 0 in both static and dynamic states. This customer (node 24) will be served by ground vehicle 11 following optimization. Thus, the values of x_{13-24}^{11} and x_{24-0}^{11} will be equal to 1 in dynamic states. After changing the solution and removing the risk link, the links in the risk zone (node 21) can be used at the time $t_r+\varepsilon$. Accordingly, aerial zone 21 is visited by drone 11 in links 17-21 to visit customers 24 through 13-4. Other aerial zones are not included in Table 8 because their assessment is not included in Fig. 15. Due to the intentional disruption, the zone's time window passing through the link of

customer 24 ($[e_4, l_4 - \delta_4]$) also changes. Additionally, the arrival time of drone 11 in zone 21 ($at_{21}{}'_{11}$) varies accordingly.

5.6. Managerial insight

The existing routing approaches in the literature determine the transportation routes of valuable goods based on historical data. However, risk estimation and route selection based solely on historical data may be unreliable. In reality, the robber may choose routes that were deemed low-risk during the planning phase (due to lack of historical data). As a result, relying on historical data to route valuable goods is insufficient. Drone surveillance is used in this study to ensure the security of valuable goods being transported. If travel planning is associated with error and risk, this approach allows for identifying potential risks and preventing an incident. For example, a ground vehicle is transporting cash, and a robber is ambushed along the vehicle's route. Assume the drone is successful in identifying the danger. In that case, it will avoid financial loss and other damages to ground vehicles and people in the vicinity of the incident and delays in delivering valuable goods to customers, and costs associated with social security violations. Thus, when compared to the high costs imposed on the transportation system by an armed robber, the costs of using drones and spending time are financially reasonable.

Due to intentional disruption and armed robbers on the route, optimization must be performed under dynamic conditions quickly. As a result, this study attempted to develop an algorithm with a short execution time. To this end, the proposed algorithm is relatively fast and high-quality compared to the literature.

6. Conclusion

In this study, a new routing problem with drones termed IRS was proposed to surveil transportation routes using drones. Due to its intrinsic nature, the transportation of valuable goods is always associated with intentional disruption (including robbery). To this end, the IRS relied on the ground fleet to transport valuable goods, while drones surveilled ground links to ensure their security. In other words, the ground vehicle could not depart from a point leading to a bank unless drones had previously ensured the security of this link.

While ground vehicles travel through customer locations, drones operate in aerial zones. A drone's surveillance and assessment must occur within a specified time before the ground vehicle departs. Additionally, if the time windows of ground points overlap, multiple drones could visit the same zone concurrently. Furthermore, if drones detect a threat via the cameras and sensors mounted on them, the SCR is notified, and an optimization process is initiated by removing the riskiest link from the transportation network (link with identified robber).

The proposed scenario was compared to two other similar ones to be evaluated. The transportation costs of all three scenarios were calculated and compared for various small-scale problems.

According to the results, the proposed problem's transportation costs are less than those of the two other scenarios.

An ALNS algorithm incorporating SA, termed D-SALNS, was developed to address the proposed problem. The proposed algorithm was evaluated on problems of various sizes. According to the small-size results, the D-SALNS algorithm can compete with the BARON solver included with commercial GAMS software. Moreover, based on the results of problems involving large-size problems, this algorithm is faster and more accurate than the classic version.

A future recommendation could consider solving the proposed problem using a multi-graph network. Charging stations can also be included to improve the transportation network's efficiency. Additionally, the proposed approach can be enhanced by including the unpredictability of routes.

7. References

Allahyari, S., Yaghoubi, S., Van Woensel, T., 2021a. A novel risk perspective on location-routing planning: An application in cash transportation. Transp. Res. E Logist. Transp. Rev. 150, 102356.

Allahyari, S., Yaghoubi, S., Van Woensel, T., 2021b. The secure time-dependent vehicle routing problem with uncertain demands. Comput. Oper. Res. 131, 105253.

Alotaibi, K. A., Rosenberger, J. M., Mattingly, S. P., Punugu, R. K., Visoldilokpun, S., 2018. Unmanned aerial vehicle routing in the presence of threats. Comput. Ind. Eng. 115, 190-205.

Boccia, M., Masone, A., Sforza, A., Sterle, C., 2021. A column-and-row generation approach for the flying sidekick travelling salesman problem. Transp. Res. C: Emerg. Technol. 124, 102913.

Bozkaya, B., Salman, F. S., Telciler, K., 2017. An adaptive and diversified vehicle routing approach to reducing the security risk of cash-in-transit operations. Networks 69(3), 256-269.

Coelho, B. N., Coelho, V. N., Coelho, I. M., Ochi, L. S., Haghnazar K, R., Zuidema, D., Lima, M. S. F., da Costa, A. R., 2017. A multi-objective green UAV routing problem. Comput. Oper. Res. 88, 306-315.

Constantino, M., Mourão, M. C., Pinto, L. S., 2017. Dissimilar arc routing problems. Networks 70(3), 233-245.

Dayarian, I., Savelsbergh, M., Clarke, J.-P., 2020. Same-day delivery with drone resupply. Transp. Sci. 54(1), 229-249.

Demir, E., Bektaş, T., Laporte, G., 2012. An adaptive large neighborhood search heuristic for the Pollution-Routing Problem. Eur. J. Oper. Res. 223(2), 346-359.

Dorling, K., Heinrichs, J., Messier, G. G., Magierowski, S., 2016. Vehicle routing problems for drone delivery. IEEE Trans. Syst. Man Cybern. Syst. 47(1), 70-85.

Ermağan, U., Yıldız, B., Salman, F. S., 2022. A learning based algorithm for drone routing. Comput. Oper. Res. 137, 105524.

Euchi, J., Sadok, A., 2021. Hybrid genetic-sweep algorithm to solve the vehicle routing problem with drones. Phys. Commun. 44, 101236.

Fallahtafti, A., Ardjmand, E., Young, W. A., Weckman, G. R., 2021. A multi-objective two-echelon location-routing problem for cash logistics: A metaheuristic approach. Appl. Soft Comput. 111, 107685.

Ghannadpour, S. F., Zandiyeh, F., 2020a. An adapted multi-objective genetic algorithm for solving the cash in transit vehicle routing problem with vulnerability estimation for risk quantification. Eng. Appl. Artif. Intell. 96, 103964.

Ghannadpour, S. F., Zandiyeh, F., 2020b. A new game-theoretical multi-objective evolutionary approach for cash-in-transit vehicle routing problem with time windows (A Real life Case). Appl. Soft Comput. 93, 106378.

Goeke, D., Schneider, M., 2015. Routing a mixed fleet of electric and conventional vehicles. Eur. J. Oper. Res. 245(1), 81-99.

Gu, Q., Fan, T., Pan, F., Zhang, C., 2020. A vehicle-UAV operation scheme for instant delivery. Comput. Ind. Eng. 149, 106809.

Guo, F., Huang, Z., Huang, W., 2021. Heuristic approaches for a vehicle routing problem with an incompatible loading constraint and splitting deliveries by order. Comput. Oper. Res. 134, 105379.

Hoogeboom, M., Dullaert, W., 2019. Vehicle routing with arrival time diversification. Eur. J. Oper. Res. 275(1), 93-107.

Karak, A., Abdelghany, K., 2019. The hybrid vehicle-drone routing problem for pick-up and delivery services. Transp. Res. C: Emerg. Technol. 102, 427-449.

Karim, S., Zhang, Y., Laghari, A. A., Asif, M. R. Image processing based proposed drone for detecting and controlling street crimes. 2017 IEEE 17th International Conference on Communication Technology (ICCT), 2017. IEEE, 1725-1730.

Kitjacharoenchai, P., Min, B.-C., Lee, S., 2020. Two echelon vehicle routing problem with drones in last mile delivery. Int. J. Prod. Econ. 225, 107598.

Kuhn, H., Schubert, D., Holzapfel, A., 2021. Integrated order batching and vehicle routing operations in grocery retail – A General Adaptive Large Neighborhood Search algorithm. Eur. J. Oper. Res. 294(3), 1003-1021.

Kuo, R. J., Lu, S.-H., Lai, P.-Y., Mara, S. T. W., 2022. Vehicle routing problem with drones considering time windows. Expert Syst. Appl. 191, 116264.

Lee, S., Jain, S., Yuan, Y., Zhang, Y., Yang, H., Liu, J., Son, Y.-J., 2019. Design and development of a DDDAMS-based border surveillance system via UVs and hybrid simulations. Expert Syst. Appl. 128, 109-123.

Lei, D., Cui, Z., Li, M., 2022. A dynamical artificial bee colony for vehicle routing problem with drones. Eng. Appl. Artif. Intell. 107, 104510.

Li, H., Wang, H., Chen, J., Bai, M., 2020. Two-echelon vehicle routing problem with time windows and mobile satellites. Transp. Res. B: Methodol. 138, 179-201.

Liu, Y., 2019. An optimization-driven dynamic vehicle routing algorithm for on-demand meal delivery using drones. Comput. Oper. Res. 111, 1-20.

Michallet, J., Prins, C., Amodeo, L., Yalaoui, F., Vitry, G., 2014. Multi-start iterated local search for the periodic vehicle routing problem with time windows and time spread constraints on services. Comput. Oper. Res. 41, 196-207.

Mohri, S. S., Asgari, N., Zanjirani Farahani, R., Bourlakis, M., Laker, B., 2020. Fairness in hazmat routing-scheduling: A bi-objective Stackelberg game. Transp. Res. E Logist. Transp. Rev. 140, 102006.

Ngueveu, S. U., Prins, C., Calvo, R. W. 2009. A hybrid tabu search for the m-peripatetic vehicle routing problem. Matheuristics. Springer.

Ngueveu, S. U., Prins, C., Calvo, R. W., 2010. Lower and upper bounds for the m-peripatetic vehicle routing problem. 4OR 8(4), 387-406.

Ngueveu, S. U., Prins, C., Wolfler Calvo, R., 2013. New lower bounds and exact method for the m-PVRP. Transp. Sci. 47(1), 38-52.

Nichols, G., 2020. Best security and surveillance drones for business in 2020: Impossible Aerospace, Microdrones, DJI, and more [Online]. Available: https://www.zdnet.com/article/best-security-surveillance-drones-for-business/

PIANA, C.,2017. The Use of UA in Private Security

Poikonen, S., Golden, B., 2020a. The mothership and drone routing problem. INFORMS J. Comput. 32(2), 249-262.

Poikonen, S., Golden, B., 2020b. Multi-visit drone routing problem. Comput. Oper. Res. 113, 104802.

Poikonen, S., Wang, X., Golden, B., 2017. The vehicle routing problem with drones: Extended models and connections. Networks 70(1), 34-43.

Radojičić, N., Djenić, A., Marić, M., 2018. Fuzzy GRASP with path relinking for the Risk-constrained Cash-in-Transit Vehicle Routing Problem. Appl. Soft Comput. 72, 486-497.

Sacramento, D., Pisinger, D., Ropke, S., 2019. An adaptive large neighborhood search metaheuristic for the vehicle routing problem with drones. Transp. Res. C: Emerg. Technol. 102, 289-315.

Schermer, D., Moeini, M., Wendt, O., 2019a. A hybrid VNS/Tabu search algorithm for solving the vehicle routing problem with drones and en route operations. Comput. Oper. Res. 109, 134-158.

Schermer, D., Moeini, M., Wendt, O., 2019b. A matheuristic for the vehicle routing problem with drones and its variants. Transp. Res. C: Emerg. Technol. 106, 166-204.

Semiz, F., Polat, F., 2020. Solving the area coverage problem with UAVs: A vehicle routing with time windows variation. Robot. Auton. Syst. 126, 103435.

Shaw, P. Using constraint programming and local search methods to solve vehicle routing problems. International conference on principles and practice of constraint programming, 1998. Springer, 417-431.

Song, B. D., Park, K., Kim, J., 2018. Persistent UAV delivery logistics: MILP formulation and efficient heuristic. Comput. Ind. Eng. 120, 418-428.

Soriano, A., Vidal, T., Gansterer, M., Doerner, K., 2020. The vehicle routing problem with arrival time diversification on a multigraph. Eur. J. Oper. Res. 286(2), 564-575.

Taguchi, G., Wu, Y., 1980. Introduction to Off-Line Quality Control, Central Japan Quality Control Association. Available from American Supplier Institute 32100.

Talarico, L., Sörensen, K., Springael, J., 2015a. The k-dissimilar vehicle routing problem. Eur. J. Oper. Res. 244(1), 129-140.

Talarico, L., Sörensen, K., Springael, J., 2015b. Metaheuristics for the risk-constrained cash-in-transit vehicle routing problem. Eur. J. Oper. Res. 244(2), 457-470.

Talarico, L., Sörensen, K., Springael, J., 2017a. A biobjective decision model to increase security and reduce travel costs in the cash-in-transit sector. Int. Trans. Oper. Res. 24(1-2), 59-76.

Talarico, L., Springael, J., Sörensen, K., Talarico, F., 2017b. A large neighbourhood metaheuristic for the risk-constrained cash-in-transit vehicle routing problem. Comput. Oper. Res. 78, 547-556.

Tamke, F., Buscher, U., 2021. A branch-and-cut algorithm for the vehicle routing problem with drones. Transp. Res. B: Methodol. 144, 174-203.

Tikani, H., Setak, M., Demir, E., 2020. Multi-objective periodic cash transportation problem with path dissimilarity and arrival time variation. Expert Syst. Appl., 114015.

Tikani, H., Setak, M., Demir, E., 2021. A risk-constrained time-dependent cash-in-transit routing problem in multigraph under uncertainty. Eur. J. Oper. Res. 293(2), 703-730.

Wang, X., Poikonen, S., Golden, B., 2017. The vehicle routing problem with drones: Several worst-case results. Optim. Lett. 11(4), 679-697.

Wang, Z., Sheu, J.-B., 2019. Vehicle routing problem with drones. Transp. Res. B: Methodol. 122, 350-364.

Xu, G., Li, Y., Szeto, W., Li, J., 2019. A cash transportation vehicle routing problem with combinations of different cash denominations. Int. Trans. Oper. Res. 26(6), 2179-2198.

Yaacoub, J.-P., Salman, O., 2020. Security Analysis of Drones Systems: Attacks, Limitations, and Recommendations. Internet of Things 100218.

Yan, S., Wang, S.-S., Wu, M.-W., 2012. A model with a solution algorithm for the cash transportation vehicle routing and scheduling problem. Comput. Ind. Eng. 63(2), 464-473.

Yu, V. F., Jodiawan, P., Gunawan, A., 2021. An Adaptive Large Neighborhood Search for the green mixed fleet vehicle routing problem with realistic energy consumption and partial recharges. Appl. Soft Comput. 105, 107251.

Zhen, L., Li, M., Laporte, G., Wang, W., 2019. A vehicle routing problem arising in unmanned aerial monitoring. Comput. Oper. Res. 105, 1-11.